

Active Wake Control by Pitch Adjustment

Analysis of field measurements

K. Boorsma

August 2015

ECN-E--15-042



Acknowledgement

This work is subsidized by the FLOW programme under project number 5.1440. Leo Machielse is acknowledged for providing his analysis of the measured field data. Edwin Bot, Arno vd Werff and Gerard Schepers are acknowledged for their assistance during interpretation of the results.

Abstract

This report gives a description of part of the work done within the framework of the FLOW project on Active Wake Control. Hereto, available field measurements at the ECN wind turbine test site EWTW are analyzed. The report is a follow up of, and largely based on a previous report on this topic [3], now extended with data from all available turbines in a row.

An increase in combined power is observed for the wake situation, i.e. when the downwind turbine is located downstream of the upwind located turbine. This increase amounts to roughly 8% for a 2° pitch angle, and is limited to the optimum tip speed ratio regime. It should be noted that this figure holds for this row of turbines only and is not necessarily representative for a farm configuration. A quantitative comparison of the different pitch angle settings is hampered by the limited size of the datasets and the fact that the turbulence intensity is not equal for the different configurations. In addition to that, the resulting power of the waked turbines will not only be influenced by the the lower incident wind speed, but also by a different tip speed ratio and corresponding C_p due to the control configuration of the turbines under consideration.

For the loads, presented in terms of flat- and edgewise fatigue equivalent blade root moments, the effect of pitch angle adjustment is as expected mostly present in the flatwise component. Reductions in the order of 10% for the downwind turbine are measured at a 2° pitch angle of the upwind turbine, which occur for the higher wind velocities. As for the power results, a quantitative comparison of the different pitch angle settings is hampered by the limited size of the datasets together with variations of the turbulence intensity.

To reduce the standard error of the field data and correct for turbulence intensity variations, it is recommended to obtain more measurements. To increase the available data for pitch angle configurations, it would be beneficial if the wind turbines can be operated at a specified pitch angle for a limited time period. Furthermore it is recommended to extend the results from the current row of turbines to a representative farm configuration (number of turbines and their respective distance). To come to a conclusion on the overall benefits of the active wake control concept, a large wind farm experiment seems to be the way forward.

Although the information contained in this report is derived from reliable sources and reasonable care has been taken in the compiling of this report, ECN cannot be held responsible by the user for any errors, inaccuracies and/or omissions contained therein, regardless of the cause, nor can ECN be held responsible for any damages that may result therefrom. Any use that is made of the information contained in this report and decisions made by the user on the basis of this information are

for the account and risk of the user. In no event shall ECN, its managers, directors and/or employees have any liability for indirect, non-material or consequential damages, including loss of profit or revenue and loss of contracts or orders.



Contents

1	Introduction	7
2	EWTW	9
3	Data reduction	11
3.1	Filtering	11
3.2	Correction for atmospheric conditions	12
3.3	Power coefficients and fatigue equivalent moments	12
3.4	Pitch angle configurations	13
3.5	Bin averaging	13
4	Results	15
4.1	General observations	15
4.2	Power	18
4.3	Loads	28
5	Conclusions and recommendations	33
A	SQL scripts	37
A.1	Power (T5-9)	37
A.2	Loads (T5-6)	41
B	Data reduction logs	45
B.1	Power (T5-9)	45
B.2	Loads (T5-6)	49
C	Data reduction figures	59

C.1	Power (T5-9)	59
C.2	Loads (T5-6)	68

1

Introduction

ECN holds a patent for the Active Wake control concepts, which aim at optimizing farm performance through active control of the turbine wake. 'Heat and Flux' farm control is a part of this concept that aims at maximizing the power output of a wind farm by adjusting the axial induction of the windward turbines below their individual optimum for power production. This will reduce the velocity deficit and turbulence in the wake and increase the output of the downwind turbines. Other benefits are decreased average loading of the upwind turbines and decreased fatigue loading of the turbines in the wake.

The reported activities aimed at the quantification of the effects of 'Heat and Flux' farm control. To this end field measurements at the ECN Wind Turbine Test Site Wieringermeer (EWTW) are analyzed from December 2004 until April 2009. These field measurements have been analyzed before in [8, 2, 3]. Questions regarding the validity and usability of these results have initiated the current study.

First, the test site is described in section 2. The adopted data reduction procedure is highlighted in section 3. The results are discussed in section 4 followed by conclusions and recommendations.

2

EWTW

The EWTW farm [6] consists of a row of five 2500 kW turbines with variable speed-pitch regulated control. These turbines have a rotor diameter and hub height of 80 m and are placed at mutual distances of 3.8 rotor diameters (D). The EWTW farm is very well suited for investigation into effects at full scale because of its state of the art turbines and the comprehensive and reliable measurement infrastructure for turbine and meteorological data.

The farm is orientated from west to east (95-275°), see Figure 1. All turbines (T5 to T9) have been used for the analysis in this report as turbine 5 is exposed to the prevailing westerly winds. Turbine 6 has been instrumented with blade root strain gauges and hence is used for the loads analysis. In addition to that a variety of signals is measured on all turbines, including electric power, nacelle wind speed and direction (both absolute nacelle direction as well as the direction of the wind vane), rotor speed and blade pitch angle. The wind characteristics are measured with the meteorological tower at 3.5D distance south-east of turbine 5 and 2.5D south-west of turbine 6. This mast measures wind speed and direction at three different heights including hub height. Also air pressure and temperature are measured at this height. The analyzed measurements at EWTW have been obtained from the period December 2004 until June 2011.

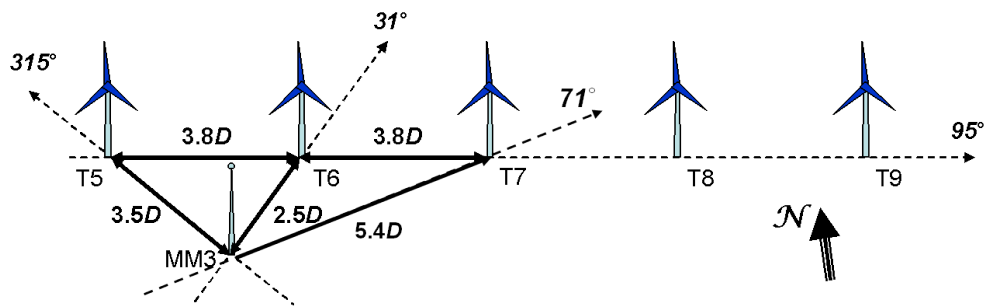


Figure 1: Main dimensions and directions in the EWTW farm. T5 to T9 are the turbine positions, MM3 indicates the measurement mast. Dimensions are expressed in rotor diameters D .

3

Data reduction

The signals of turbine 5 to 9 together with the meteorological data from mast 3 have been used for the analysis in this report. 2-, 5- and 10-minute statistics have been retrieved from the data base. The 2-minute SQL-scripts for this purpose can be found in appendix A. Wind direction (between 200 and 300°), operational mode (between 10.5 and 14.5) and minimum power (>25 kW) of turbine 6 are used as filter criteria in these scripts.

Since load measurements have only been performed on Turbine 6, a distinguishment is made between the data reduction for the loads and the power performance study. For the loads study, a common dataset consisting of only turbine 5 and 6 is under consideration. For the power performance study, a common data set using the measurements of all 5 turbines are used. Requiring valid signals for all turbines at the same time stamp significantly reduces the available data points for this last data set. Therefore only 2 minute averages are used for this study.

3.1 Filtering

After retrieving the statistics from the database, a second data reduction step is performed to filter out erroneous samples and outliers. These steps are outlined below. For more details, please consult appendix B which contains a summary of the results of this procedure.

Non-numeric values The misalignment of the turbine is calculated by means of subtracting the average wind direction measured by the meteo mast from the average nacelle direction. In some cases the nacelle direction is not recorded, resulting in a non-numeric value (NaN). These values are excluded from the dataset. The same holds for samples with NaN values of air pressure ('Pair') and flat and edgewise moments ('Mflat' and 'Medge').

Power Only normal operation conditions below rated wind speed are considered. Although the operational mode and minimum power for turbine 6 has already been filtered by the SQL script, the minimum average power of turbine 5 is also filtered to be larger than 25 kW.

Nacelle direction standard deviation The standard deviation of the nacelle direction indicates to what extent the turbine has been yawing during the sample. Samples have been excluded for standard deviation exceeding 15°.

Average wind speed Although operational mode and minimum power filters should have excluded unsuitable samples, the average wind speed has also been restricted between 5 and 15 m/s.

Nacelle to wind speed ratio The wind speed is measured at the meteo mast located 3.5 diameters distance from the turbine. There can be differences between the wind that is experienced by the turbine and the meteo mast. Since the wind speed at the meteo mast is used to correlate with the turbine measurements, ratios between average nacelle and wind speed are restricted between 0.85 and 1.15.

Turbulence intensity The turbulence intensity can be calculated by dividing the standard deviation of the wind speed over its average, both measured at the meteo mast. Extremely low and high values are filtered out by restricting this value between 1% and 20%

Pitch angle variation Even during normal operation pitch angles can vary. The difference between the maximum and minimum pitch angle of a data set is restricted to 0.2°.

3.2 Correction for atmospheric conditions

Power, edgewise and flatwise moments scale different with atmospheric conditions. The edgewise moment is dictated by gravity forces and the flatwise moment by aerodynamic force. The latter is influenced by atmosphere linearly through air density. The variation of the air density can be shown to lie between 1.18 and 1.28 kgm⁻³ for the selected samples. This is regarded as a small variation and hence the influence of atmospheric conditions is not taken into account.

3.3 Power coefficients and fatigue equivalent moments

The power coefficient for an individual turbine can be determined using

$$C_p = P / (0.5\rho U^3 A) \quad , \quad (3.1)$$

with

C_p	[-]	power coefficient
P	[Watt]	electric power
ρ	[kgm ⁻³]	air density
U	[m/s]	wind speed
A	[m ²]	rotor area.

Here the air density ρ is calculated from the measured air pressure and temperature using the ideal gas law. To compare the power output for turbine 5 to 9 together, their values are averaged according to

$$C_{p_{park}} = \frac{1}{5} \sum_{i=5}^9 C_{p_{Ti}} \quad , \quad (3.2)$$

with

$C_{p_{park}}$ [-] averaged power coefficient
 $C_{p_{Ti}}$ [-] turbine i power coefficient.

Here, all C_p values are made dimensionless using the same wind speed as measured at the meteorological mast at hub height.

In addition to the power coefficients, the fatigue equivalent flatwise and edgewise moments of turbine 6 are acquired for two different material constants (steel and glass fibre). The rain-flow counting method was applied to the raw signal and the equivalent loads have readily been determined in the database according to IEC 61400-13 [1].

3.4 Pitch angle configurations

The filtered data is divided into several data sets using the operational pitch angle of turbine 5 and 6. Thereto a naming convention is adopted: 20000 indicates a pitch angle of 2° for the first turbine in the row from west to east (turbine 5) and 0° for turbine 6 to 9.

3.5 Bin averaging

Bin averaging is applied to the resulting data sets both in wind speed and direction. The bin averaging settings are given in Table 1. The standard error of the mean within each bin is calculated using

$$S = \sigma / \sqrt{N} \quad , \quad (3.3)$$

with

S [] standard error of bin average mean
 σ [] standard deviation of the bin data samples
 N [-] number of samples per bin.

Table 1: Bin averaging settings

	2 min average	5 min average	10 min average
Required samples per bin for valid average	12	6	2
Wind speed bins	5 to 13 m/s, $\Delta = 1$ m/s		
Wind direction bins	200° to 300°, $\Delta = 5^\circ$		
Wake sector	267° to 281°		

4

Results

The number of remaining samples of the resulting data sets are summarized in Table 2. The resulting data sets for 40xxx and 22xxx are rather small. As a result it will appear that the corresponding uncertainties for these data sets are rather large.

Table 2: Data set summary

<i>power</i>		<i>loads</i>		<i>loads</i>	<i>loads</i>
pitch config	2 min average samples [-]	pitch config	2 min average samples [-]	5 min average samples [-]	10 min average samples [-]
00000	110348	00xxx	127857	57602	28839
20000	5511	20xxx	5461	2410	1285
40000	0	40xxx	1789	897	442
22000	0	22xxx	1617	731	402

4.1 General observations

Contour plots showing the distribution of several operational variables mostly for the 00xxx and 00000 configuration are shown in appendix C (Figures 14 to 27).

Turbulence intensity

From Figure 14 and 22 it becomes clear that the majority of the collected data points are distributed in the undisturbed south westerly direction. The turbulence intensity measured by the meteorological mast increases with wind speed between 5 and 11 m/s, but appears to decrease again above 12 m/s. There is a clear directional dependence of roughly 5% difference which could be explained by the presence of obstructions in the vicinity such as villages and surrounding turbines. The turbulence intensity and all other variables displayed in appendix C.2 show only little difference between the three averaging times applied.

From previous measurements [9] it was illustrated that the variation of turbulence intensity influences the performance. This can partly be explained by the increase in available kinetic energy in the air, causing a higher effective local velocity. More important is the fact that an increased turbulence intensity enhances the flow mixture in the wake, resulting in a faster recovery of the velocity deficit. As a consequence the power of both undisturbed (upstream) and disturbed (downstream) turbines increases for an increasing turbulence intensity.

Nacelle wind speed

The nacelle windspeed is an indicator for the wind experienced by the turbine. This signal is measured by a sonic anemo-meter or in case of failure of this signal by a cup anemo-meter. The top part of Figure 23 shows the nacelle wind speed of turbine 5, which should theoretically be a flat line with wind direction. In practice a local maximum can be observed around 260° wind direction. Going back to the turbulence intensity in Figure 22, the peaks coincide with the local maximum of the turbulence intensity. Since the nacelle wind speed measurement takes place downstream of the rotor (i.e. in the rotor wake), the increased flow mixture could explain the small peaks in the nacelle wind speed.

The bottom part of Figure 23 clearly shows turbine 6 to operate in the wake of turbine 5 for westerly winds. The same holds for the standard deviation of the nacelle wind speed in Figure 24. It is noticed that the velocity standard deviation of turbine 6 decreases in the wake of turbine 5 due to the decrease in wind speed. However because of the increased turbulence in the wake of turbine 5, the standard deviation does not decrease as much as the wind speed does (relatively) and the wake affected area is less wide (direction wise).

The standard deviation of the turbine 5 nacelle wind speed does not show an entirely flat trend with wind direction. The local increase around a wind direction of 260° agrees with the direction of the maximum of the turbulence intensity from the meteorological mast.

Tip speed ratio

Figure 25 displays the tip speed ratio which is made dimensionless using the wind velocity measured by the meteorological mast. Theoretically the turbines should operate at their optimal tip speed ratio λ , since the data is filtered in the below rated region. In practice the rotational speed setting is limited by the controller, which means that the tip speed ratio (and thus the operating condition of the rotor) varies

with wind speed even below rated conditions. This is clearly visible in Figure 25. The two-dimensional plot in Figure 2 illustrates that the rpm variation with wind speed is 'flattened' before rated rpm, probably to reduce turbine loading. Because of this observation, the results are presented not only as a function of direction but also of wind speed bin.

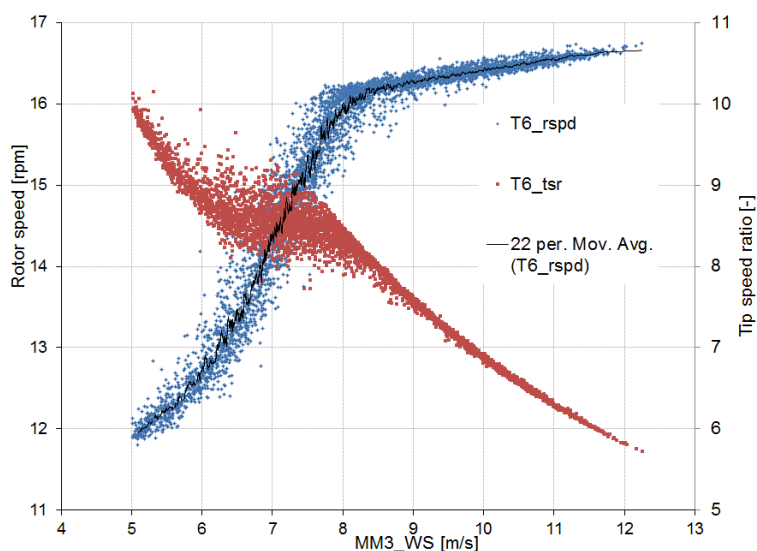


Figure 2: Variation of turbine 6 rotational speed and tip speed ratio with wind speed (measured by the meteorological mast) in undisturbed wind direction.

Figure 25 shows that for turbine 5 again the trend with wind direction is not entirely flat and the maxima at 220° , 260° and towards 300° are in agreement with the maxima of the turbulence intensity. As a consequence of the low velocities in the wake of turbine 5, the turbine 6 rotational speed decreases and with that also the calculated tip speed ratio.

Yaw misalignment

Observing the yaw (misalignment) angle in Figure 20 and 26 it should be noted that this quantity is calculated by subtracting the wind direction as measured by the meteorological mast from the measured nacelle direction at the turbine. As such the illustrated value is not necessarily a misalignment since the local wind direction might be different from the measurement at the meteorological mast, especially in the wake of the turbine.

Firstly, the resulting misalignment does not vary around 0° contrary to expectations. This has been observed previously [4, 7] and is probably caused by a faulty measurement of the nacelle direction or meteorological mast wind vane since it is not likely that the turbine continuously operates in yawed flow conditions.

For turbine 5 the misalignment is not distributed randomly but changes roughly from -4° at 200° to -7° at

300° direction. As pointed out in [5] this could well be explained by a faulty indication of meteorological mast wind direction. The wind direction vane taken for this direction range is located on a boom which is aligned at 240°. It can easily be shown that the local streamlines around the mast show direction changes up to 3° at this short distance between the vane and the mast.

The yaw angles of turbine 6 show that the side areas of the wake (just off the wake center line) show positive and negative values with a difference of approximately 10°. This could be attributed to the fact that the turbine operates in the partial wake behind turbine 5. As was previously hypothesized in [10], this can result in an asymmetric wake expansion, causing a change in local wind direction.

4.2 Power

Figure 3 illustrates the variation of combined and individual power coefficients for the 00000 configuration. Especially for the turbine 5 plot (undisturbed), it becomes clear that also here the turbulence intensity variation (Figure 10a) dictates the power coefficient variation for undisturbed wind directions. In addition to a previous hypothesis on the influence of wake rotation in partial wake [10], the peak in $C_{p_{park}}$ around 260° seems to be caused by the high turbulence intensity of this direction. The variation of power coefficient with wind direction slightly differs between the turbines, possibly indicating that turbulent inflow also varies spatially in the area considered.

Figure 4 shows line plot variations of both combined and individual power coefficient as a function of wind speed for the wake sector as defined in Table 1. Turbine 5 still experiences undisturbed conditions and due to the variation of tip speed ratio with wind speed as programmed by the controller (see also Figure 2), this curve resembles a $C_p - \lambda$ curve (although tip speed ratio decreases from right to left). For the other turbines the wake effect is most pronounced for lower wind speeds, which agrees with higher tip speed ratio and consequently higher axial induction, resulting in a lower combined power. For increasing wind speeds the induction decreases, resulting in decreasing wake effects and consequently increasing combined power coefficients.

Figure 4 also demonstrates the effect of the pitch angle on the power production. The increased pitch angle causes an almost constant decrease of power for turbine 5, as expected. For high wind velocity (low tip speed ratio) this effect diminishes, possibly because at a part of the span the amount of drag induced by separated flow (high local angle of attack) is reduced by increasing the pitch angle. Around 8 m/s a clear gain of around 8% is observed in terms of combined power performance due to the pitch adjustment. As expected, the highest gain is achieved for turbine 6, reducing further downwind. However, due to the limited number of samples for the 20000 configuration, the error bar is also quite large. For wind speeds below 7 m/s and above 9 m/s, it can be observed that the effect of pitch adjustment is disadvantageous. Plots showing the variation with wind direction for 8 m/s and 11 m/s can be found in Figure 5 and 6 respectively. To dive into the cause of the observed behaviour, Figure 7 to 9 show the variation of nacelle wind speed divided by undisturbed wind speed from the meteorological mast. The trends are in agreement with the observed variation in power. Figure 10 then shows the corresponding measured variations in turbulence intensity. It is striking to observe in Figure 10b that the turbulence

intensity variation for the wake sector agrees with the shown power and nacelle wind speed variation. Although the variations between 00000 and 20000 are less than 1% per wind speed bin, it looks like the variation cannot be neglected for the present study. This is confirmed by the results for undisturbed wind direction in appendix C.1. Theoretically, the power should be the same between the 00000 and 20000 configuration. However the displayed variation in Figure 15, largely in agreement with the turbulence intensity variation in Figure 14c shows that these variations can not be ignored. Filtering for this variable would unfortunately yield a too small dataset for statistical analysis.

In addition to that it should be noted that the non-constant tip speed ratio operation in partial load of this turbine complicates the quantification of the benefits of pitch angle adjustment. Due to the lower incident velocity in the wake, the tip speed ratio of the waked turbines (turbine 6-9) will be different from the first turbine in the row (turbine 5). Hence the resulting power will not only be lower due to the lower incident wind, but also due to a different tip speed ratio and corresponding C_p . For the first turbine operating at the optimal tip speed ratio (8 m/s), it can be argued that this will increase the gain of the pitch angle adjustment. Because the waked turbine will operate at a tip speed ratio closer to the optimum than for the situation without pitch angle adjustment, an extra performance increase is obtained. On the other hand, for high wind speeds (tip speed ratios below optimum), less wake effect by pitch adjustment will reduce the gain since the waked turbines will be further away from the optimum tip speed ratio (due to the decreased axial induction factor of the first turbine). Because power scales with the cube of wind velocity for constant C_p , the relative contribution of the effect of C_p change due to tip speed ratio will scale less fast than the effect of wind speed change on power.

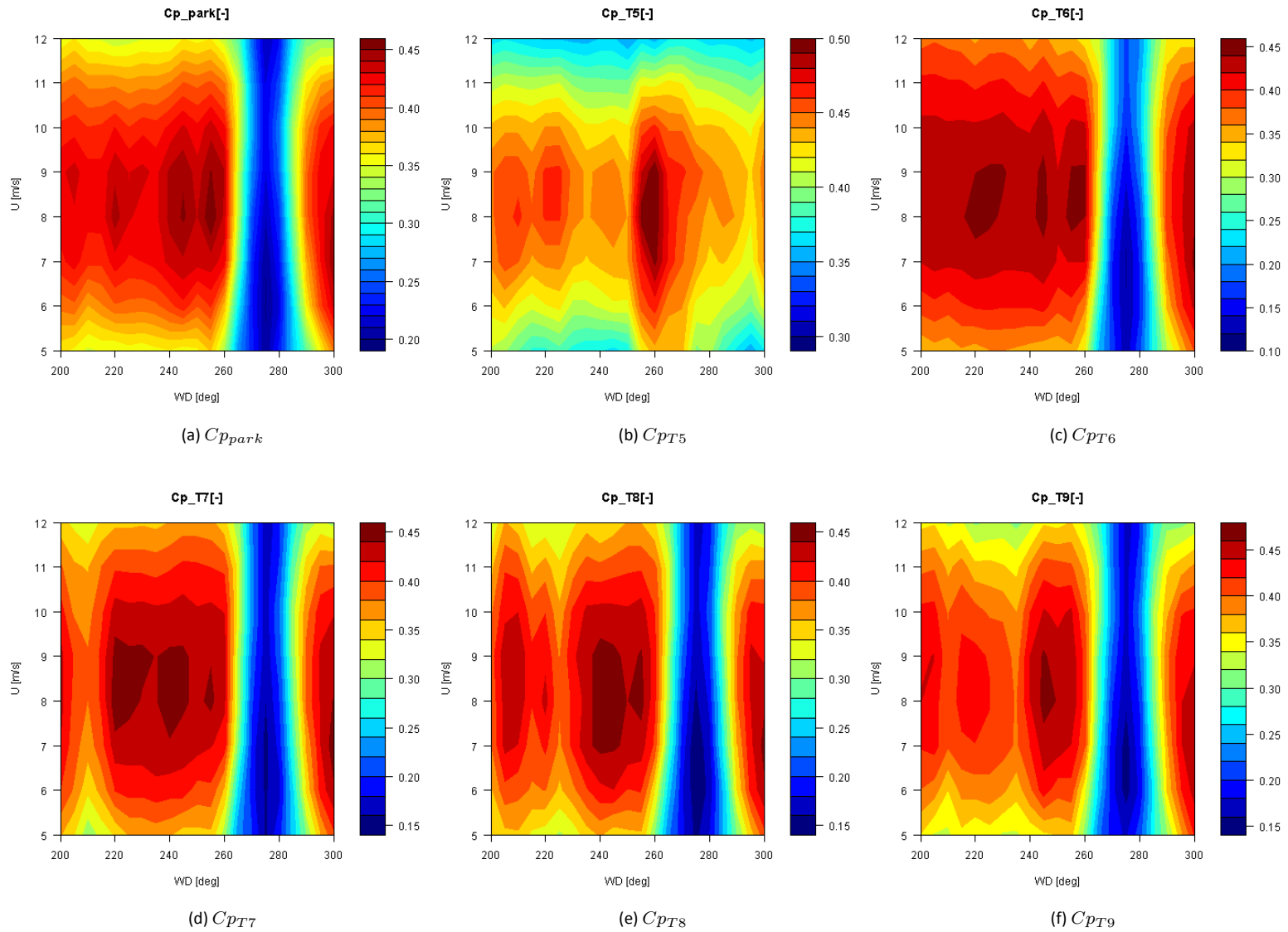


Figure 3: Contour plot of power coefficients variation for 00000, 2 minute average

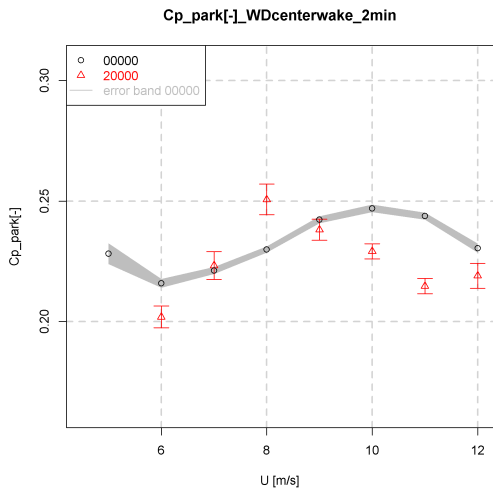
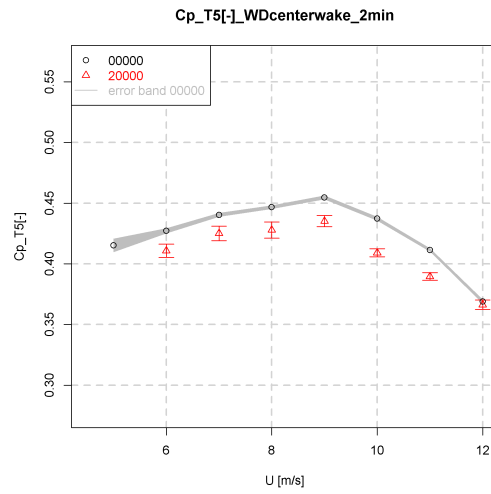
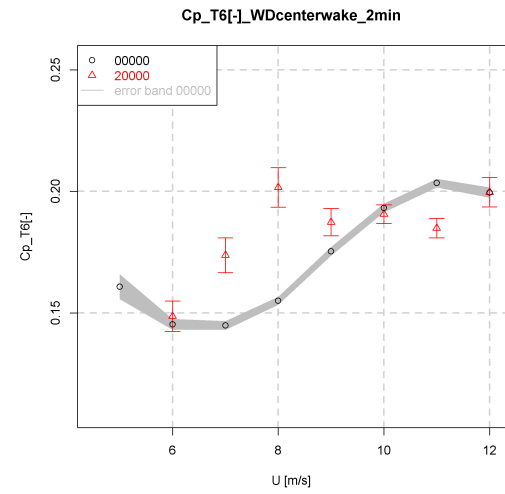
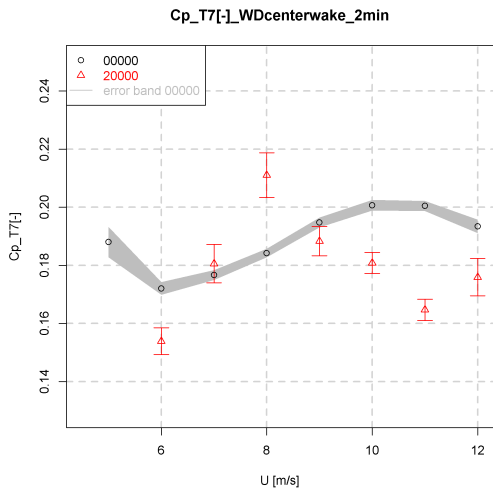
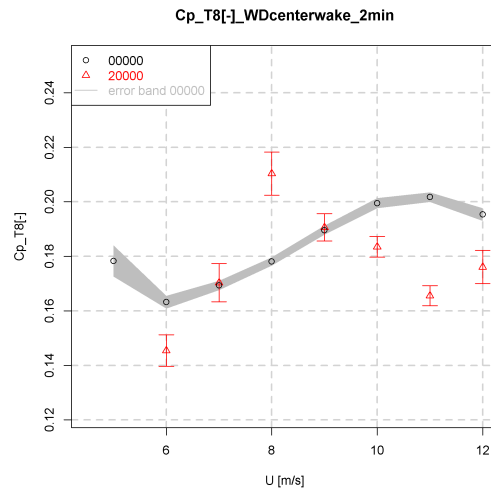
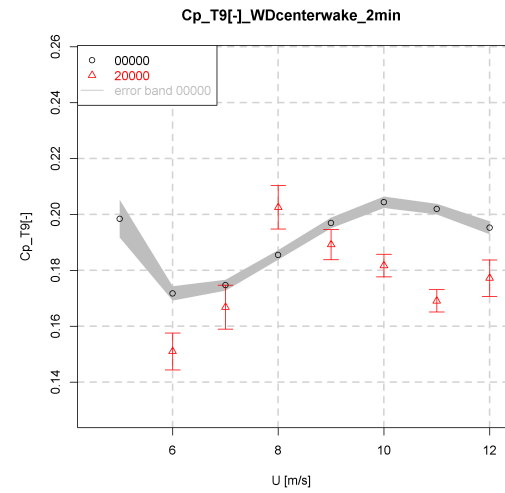

 (a) $C_{p_{park}}$

 (b) $C_{p_{T5}}$

 (c) $C_{p_{T6}}$

 (d) $C_{p_{T7}}$

 (e) $C_{p_{T8}}$

 (f) $C_{p_{T9}}$

 Figure 4: Variation of C_p with wind speed for wake sector , 2 minute average

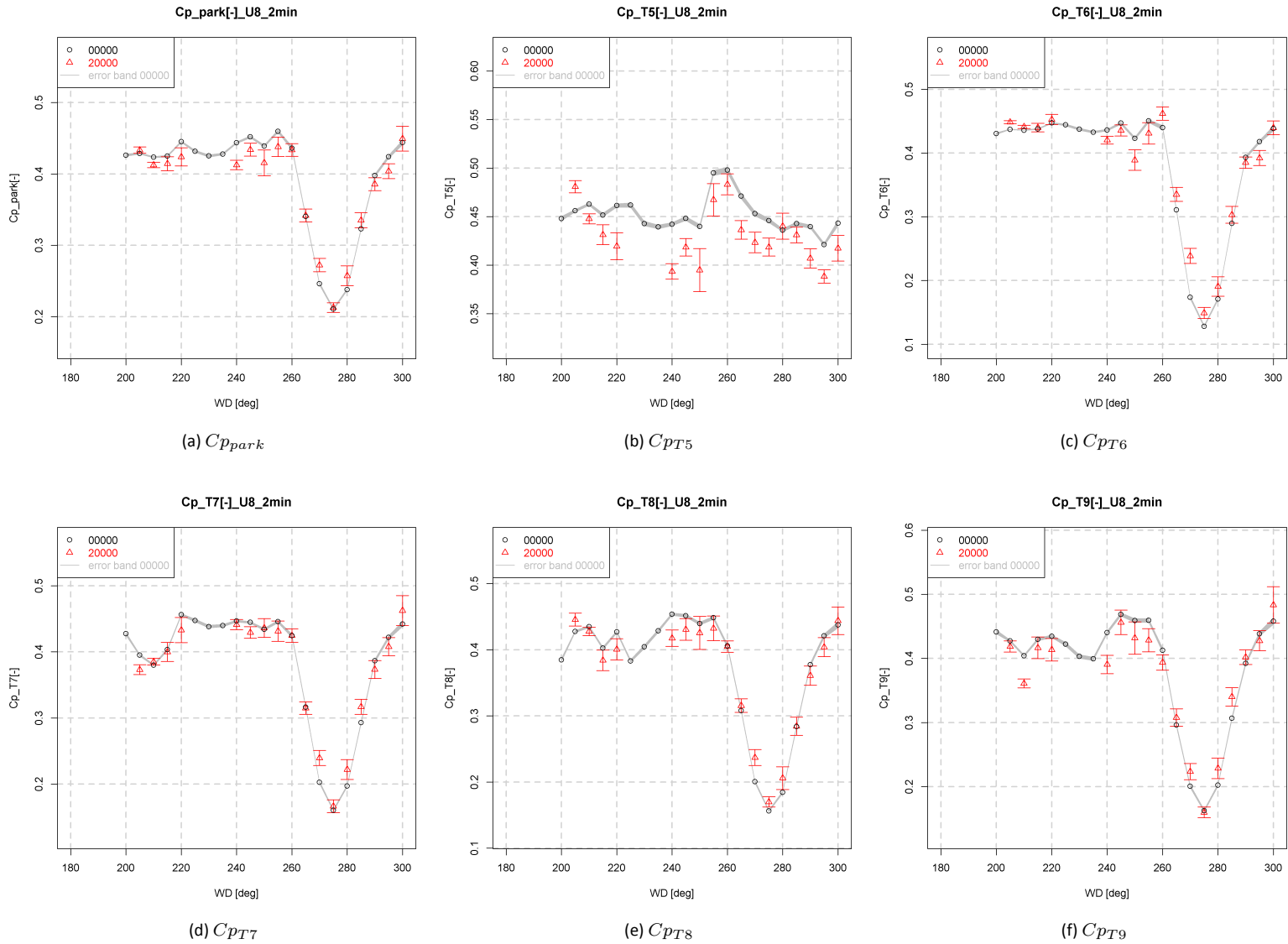
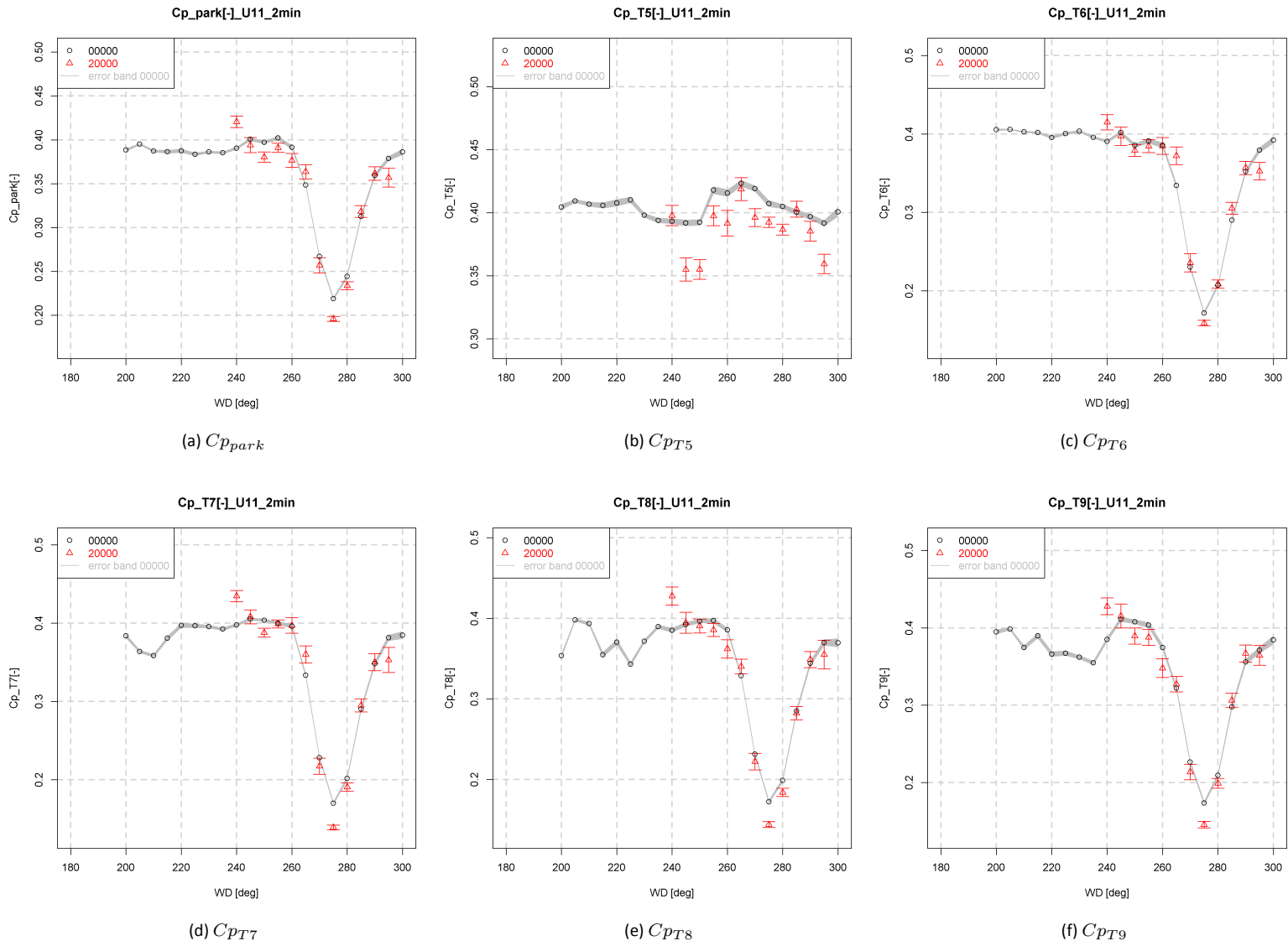


Figure 5: Variation of C_p with wind direction for $U_{bin} = 8$ m/s, 2 minute average


 Figure 6: Variation of C_p with wind direction for $U_{bin}=11$ m/s, 2 minute average

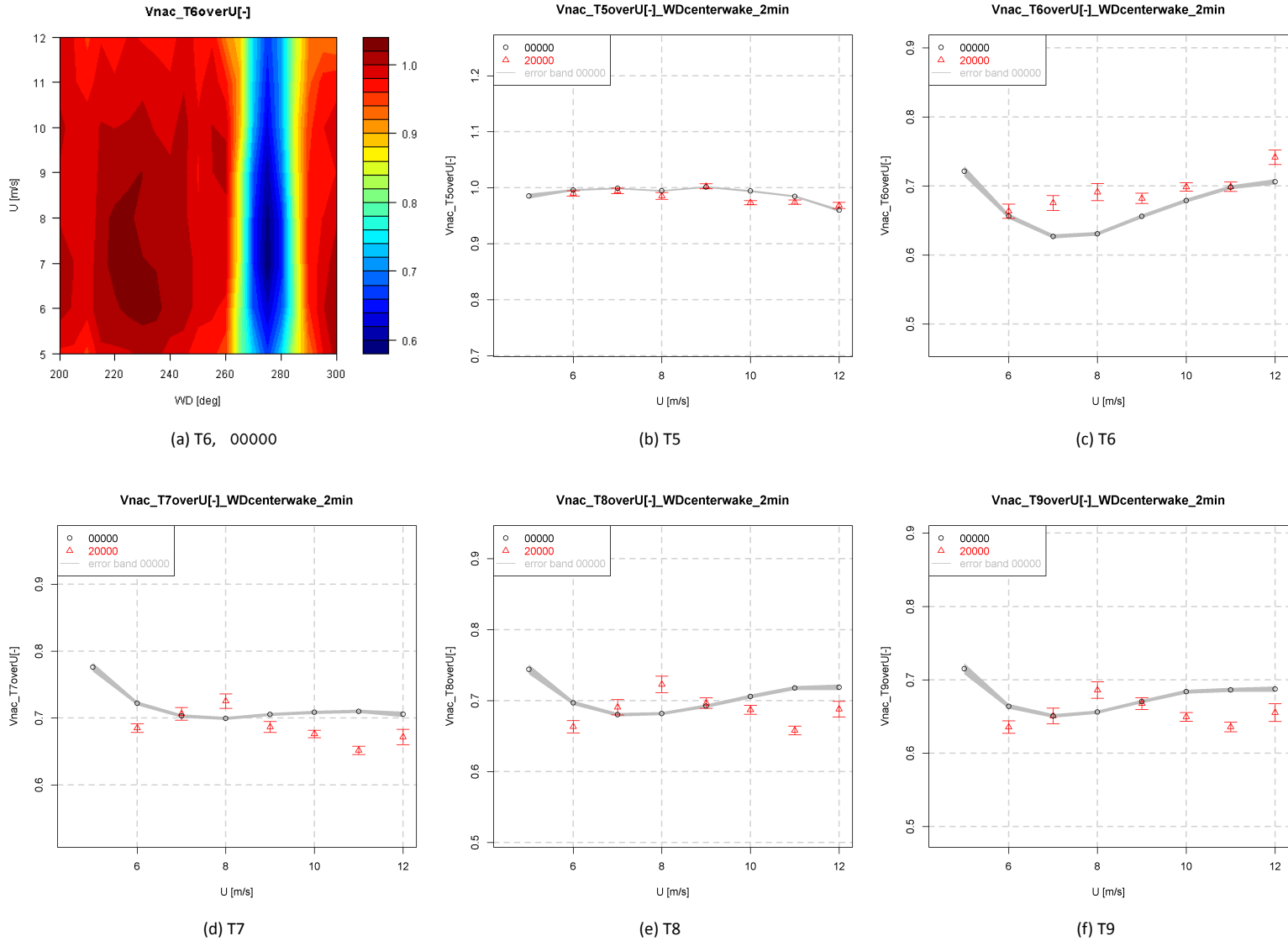


Figure 7: Variation of nacelle wind speed over meteo mast wind speed ratio with wind speed, wake sector, 2 minute average

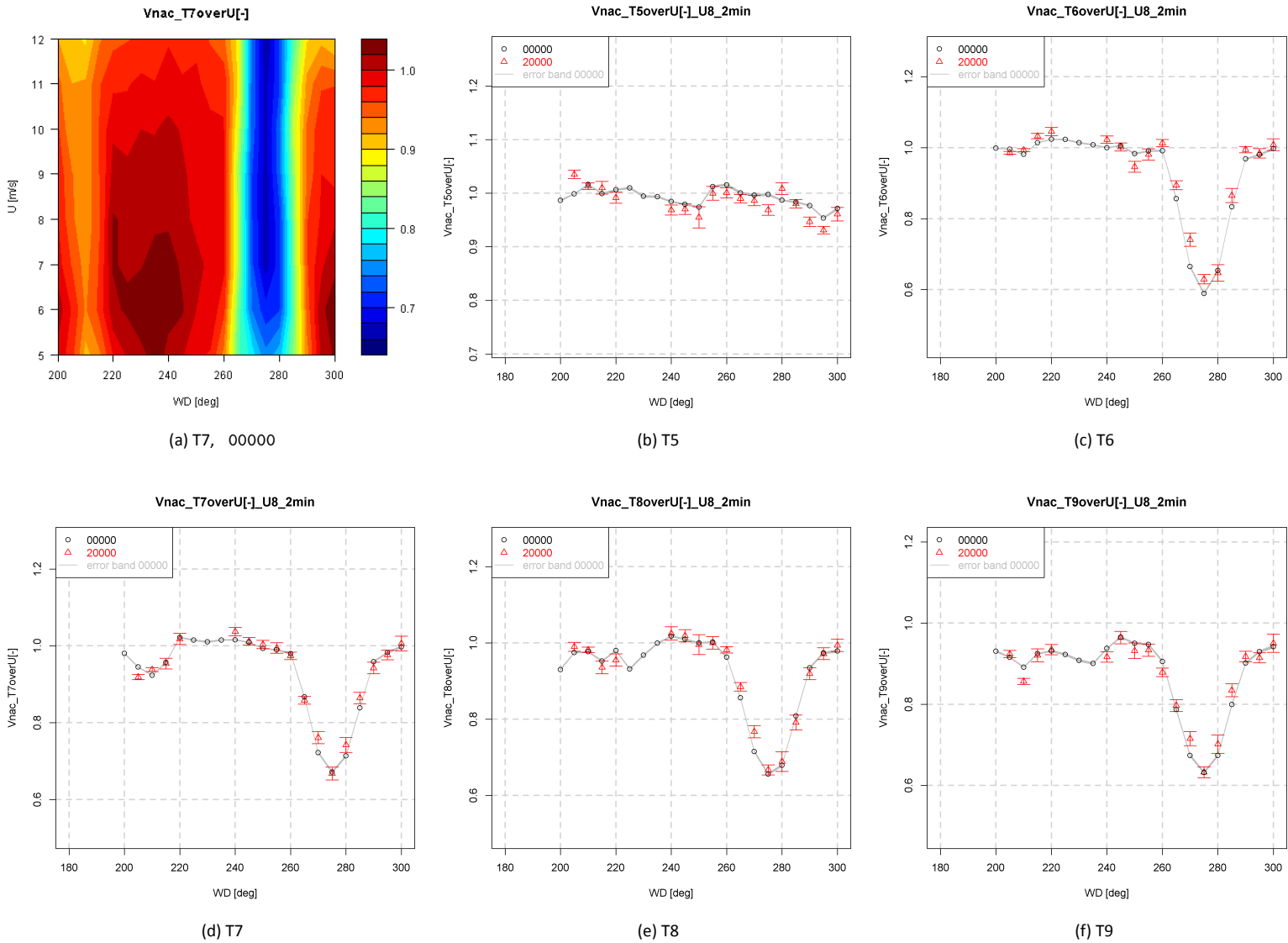


Figure 8: Variation of nacelle wind speed over meteo mast wind speed ratio with wind direction, $U_{bin} = 8$ m/s, 2 minute average

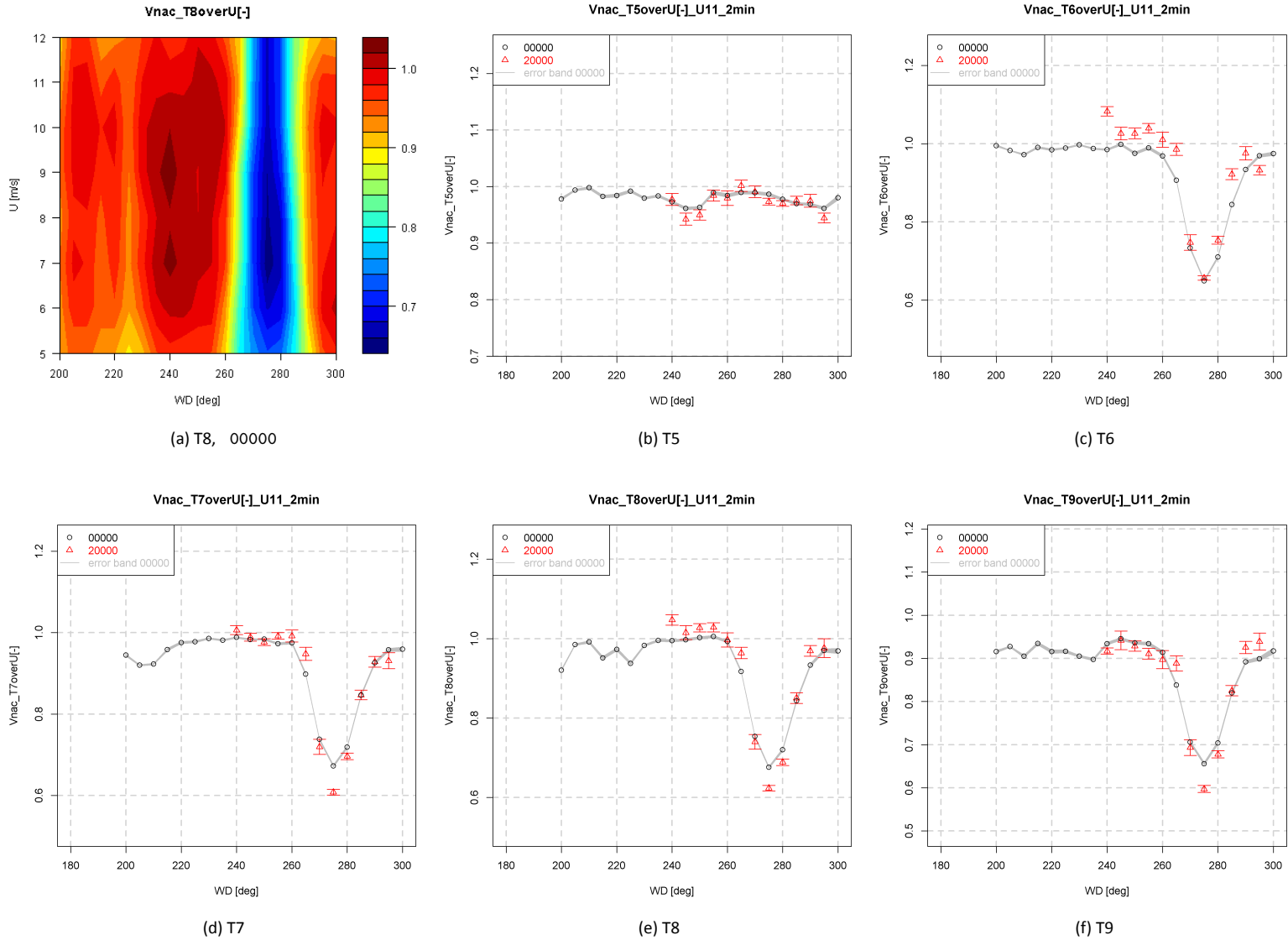


Figure 9: Variation of nacelle wind speed over meteo mast wind speed ratio with wind direction, $U_{bin} = 11$ m/s, 2 minute average

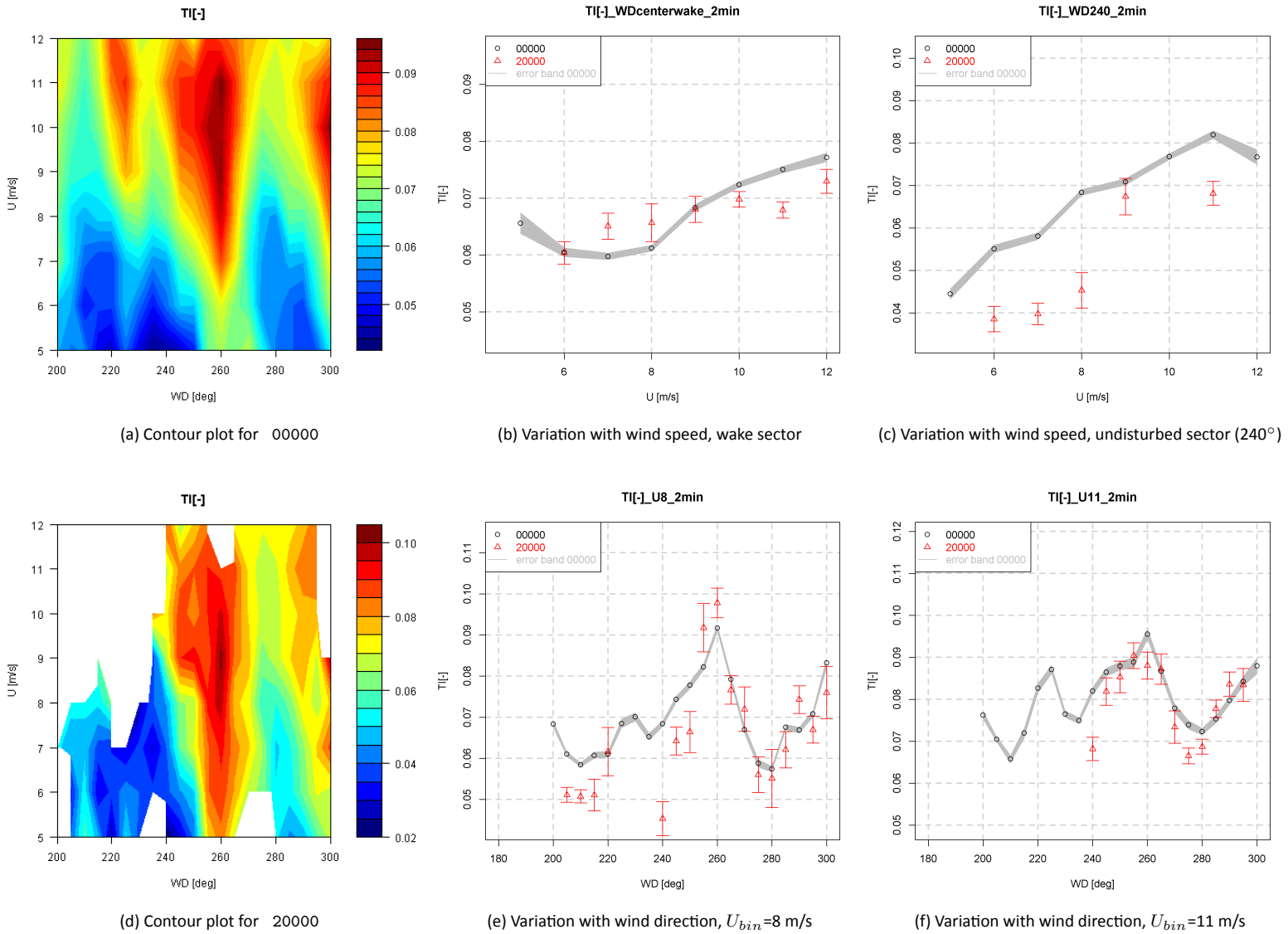


Figure 10: Variation of turbulence intensity measured by the meteo mast for several configurations, 2 minute average

4.3 Loads

The variation of flatwise fatigue equivalent loads of turbine 6 is illustrated in Figure 11. The contour plot shows a hat shape with a dent in the middle when turbine 6 is positioned directly downstream of turbine 5. This can be explained by the fact that during partial wake situation the blades sweep in and out the wake region, which induces more unsteady loads. For a full wake situation the effective wind fluctuation as experienced by the turbine is smaller. In addition to that, the highly turbulent tip vortices will pass round the rotor instead of through the rotor plane. For velocities below 7 m/s the dent seems to disappear. At these low velocities and consequently high tip speed ratios the turbine(s) start to enter the turbulent wake state, which could influence the partial and full wake situations. The increased levels at 220° wind direction and the fact that the left part of the 'hat' features higher fatigue loads can be explained by the increased turbulence intensities in these directions as illustrated in Figure 12a.

For the undisturbed wind sector (Figure 11d) the different configurations should theoretically coincide. The measured discrepancies can again be explained by turbulence intensity differences as illustrated in Figure 12d. For the wake sector the 40xxx configuration shows a large decrease, which again coincides with a higher turbulence intensity. Since an increased turbulence intensity facilitates wake mixing and a faster recovery of the wake velocity deficit, this is expected to decrease the fatigue loading in the wake of turbine 5. The question is whether changing the pitch axis of the upstream turbine or an increase in turbulence intensity is a dominant factor. For this sector however also the 20xxx configuration shows a decrease in fatigue loading, whilst turbulence intensity levels are roughly the same. Hence it appears that these gains in fatigue loading can be attributed to active wake control by pitch adjustment. Reductions are in the order of 10% and seem to occur only for the higher wind velocities (or low tip speed ratios).

The variation of edgewise fatigue equivalent loads is illustrated in Figure 13. A sine shape is observed whilst traversing through the wake where the left half shows an increase and the right half a decrease. This can be explained by the contribution of the aerodynamic torque which increases the absolute value of the edgewise moment (summation of gravitational and aerodynamic forces) for the downstroke whilst it decreases this figure for the upstroke. As such a partial wake situation on one side of the wake increases the edgewise load difference between up- and downstroke whilst on the other side it decreases the edgewise moment difference between up- and downstroke and hence the fatigue equivalent moment.

The edgewise fatigue equivalent moment is predominantly determined by gravity contributions. A very small heat and flux effect can be observed in the order of 1%, with a light preference at higher wind speeds. However the fact that similar differences can be observed for the undisturbed wind sector at 240° gives rise to speculations on the accuracy of this observation.

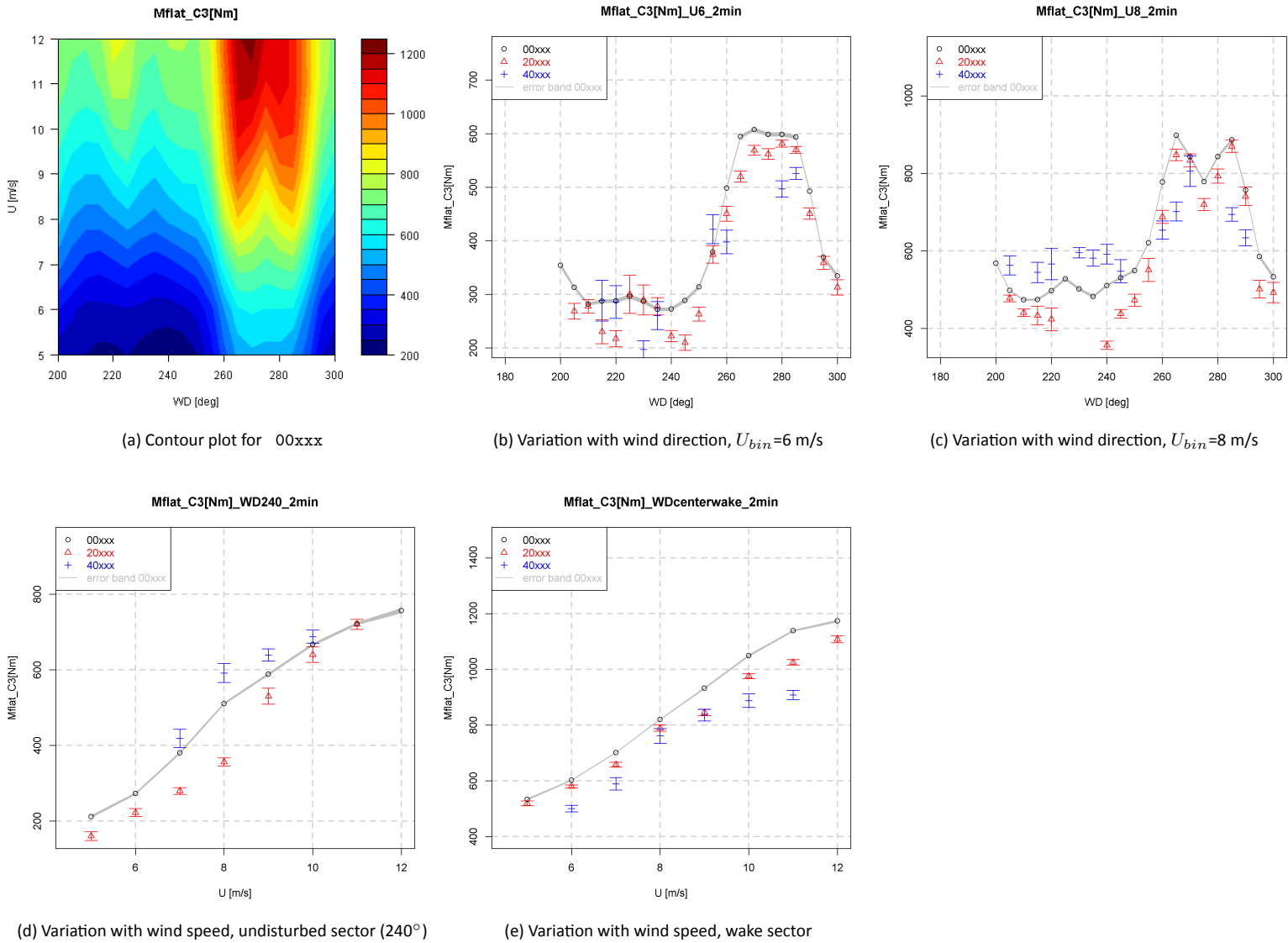


Figure 11: Variation of flatwise fatigue equivalent moment for several configurations, 2 minute average

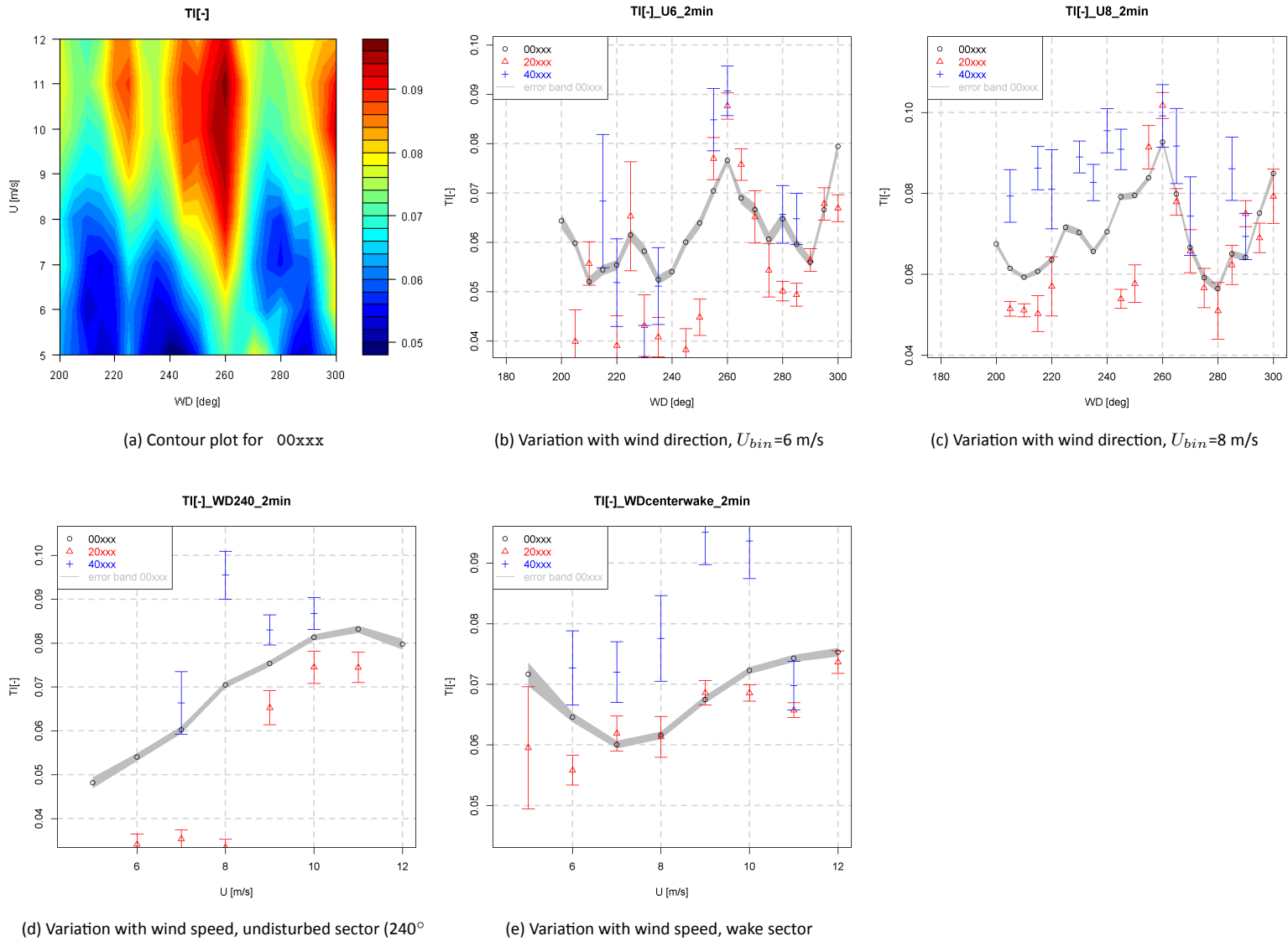


Figure 12: Variation of turbulence intensity measured by the meteo mast for several configurations, 2 minute average

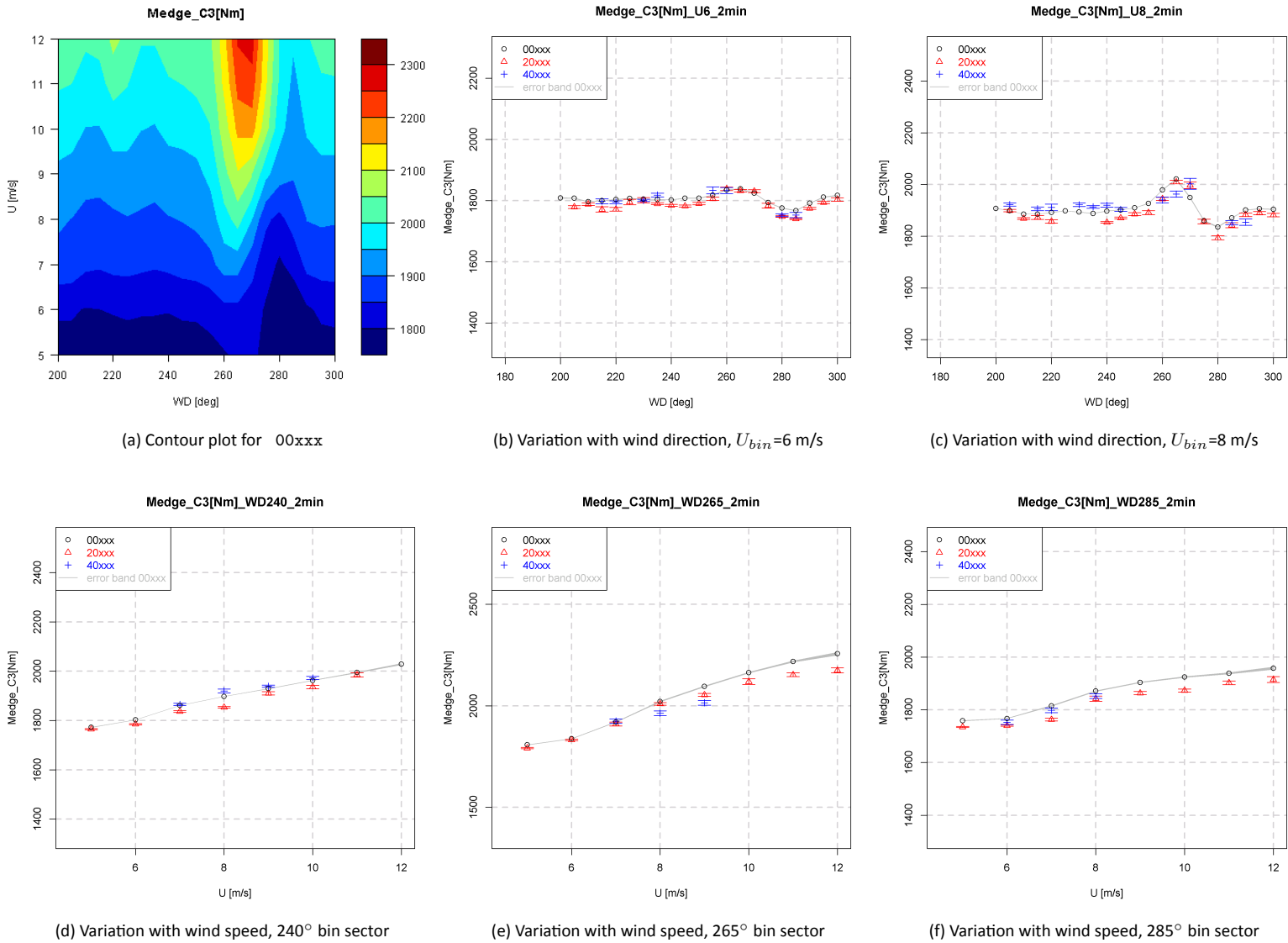


Figure 13: Variation of edgewise fatigue equivalent moment for several configurations, 2 minute average

5

Conclusions and recommendations

The effect of turbine pitch angle variation on performance and loads of a row of wind turbines is investigated using field measurements. In addition to that an attempt is made to physically clarify the measured effects in terms of loads and performance of a turbine wake impinging on downstream turbines.

An increase in combined power is observed for the wake situation, i.e. when the downwind turbine is located downstream of the upwind located turbine. This increase amounts to roughly 8% for a 2° pitch angle, and is limited to the optimum tip speed ratio regime. It should be noted that this figure holds for this row of turbines only and is not necessarily representative for a farm configuration. A quantitative comparison of the different pitch angle settings is hampered by the limited size of the datasets and the fact that the turbulence intensity is not equal for the different configurations. In addition to that, the resulting power of the waked turbines will not only be influenced by the lower incident wind speed, but also by a different tip speed ratio and corresponding C_p due to the control configuration of the turbines under consideration.

For the loads, presented in terms of flat- and edgewise fatigue equivalent blade root moments, the effect of pitch angle adjustment is as expected mostly present in the flatwise component. Reductions in the order of 10% for the downwind turbine are measured at a 2° pitch angle of the upwind turbine, which occur for the higher wind velocities (or low tip speed ratios). As for the power results, a quantitative comparison of the different pitch angle settings is hampered by the limited size of the datasets and variations of the turbulence intensity.

It is recommended to correct both power and loads for atmospheric turbulence intensity variations, since the trend is clearly influenced by this quantity. To reduce the standard error of the field data it is rec-

ommended to obtain more measurements. To increase the available data for pitch angle configurations, it would be beneficial if the wind turbines can be operated at a specified pitch angle for a limited time period.

Furthermore it is recommended to extend the results from the current row of turbines to a representative number of turbines for a farm. It should also be realised that the respective distance between the turbines is only $3.8D$ in this case, which may not always be representative for a commercial wind farm. To come to a conclusion on the overall benefits of the 'Heat and Flux' farm control concept, a large wind farm experiment seems to be the way forward.

Bibliography

- 1 IEC TS 61400-13, Wind turbine generator systems Part 13: Measurement of mechanical loads, June 2001.
- 2 S. Barth. Heat & Flux, Validation and Proof of Concept. Technical Report ECN-X-07-119, ECN, 2007.
- 3 Boorsma, K. Heat and Flux, Analysis of field measurements. Technical Report ECN-C-12-048, ECN, 2012.
- 4 Boorsma, K. Power and loads for wind turbines in yawed conditions, Analysis of field measurements and aerodynamic predictions. Technical Report ECN-C-12-047, ECN, 2012.
- 5 E.T.G. Bot. Private communication, September 2012.
- 6 P.J. Eecen et al. Measurements at the ECN wind turbine test station wieringermeer. Technical Report ECN-RX-06-055, ECN, 2006.
- 7 L.A.H. Machielse. Performance coefficients in a misaligned 2.5 MW turbine. Technical Report ECN-Wind Memo-12-012, ECN, 2012.
- 8 L.A.H. Machielse et al. Evaluation of "Heat & Flux" Farm Control, Final Report. Technical Report ECN-E-07-105, ECN, 2007.
- 9 Machielse, L.A.H. Validatiemetingen EWTW, Eindrapport. Technical Report ECN-E-06-062, ECN, 2006.
- 10 Schepers, J.G. Analysis of 4.5 years EWTW wake measurements. Technical Report ECN-E-09-057, ECN, 2009.

A

SQL scripts

A.1 Power (T5-9)

SQL script for 2 minute average data

```
select r1."t_0",
"MM3_WS80_240_2min_avg", "MM3_WS80_240_2min_std",
"MM3_WS80_240_2min_min", "MM3_WS80_240_2min_max",
"MM3_WD80_240_2min_avg", "MM3_WD80_240_2min_std",
"MM3_WD80_240_2min_min", "MM3_WD80_240_2min_max",
"MM3_Pair80_2min_avg",
"MM3_Tair80_2min_avg",

"T6_Pwsnac_2min_avg", "T6_Pwsnac_2min_std",
"T6_PEpow_2min_avg",
"T6_Pnacdrtn_2min_avg", "T6_Pnacdrtn_2min_std",
"T6_Popmode_2min_min", "T6_Popmode_2min_max",
"T6_Ppitch1_2min_min", "T6_Ppitch1_2min_max", "T6_Ppitch1_2min_avg",
"T6_Rspd_2min_avg", "T6_Rspd_2min_std",
"T6_Rspd_2min_min", "T6_Rspd_2min_max",
"MM3_WS80_true_2min_avg", "MM3_WS80_true_2min_std", "MM3_WS52_true_2min_avg", "T6_PEpow_2min_avg",

"T6_Mbe1_load_P_2min_eql_C1", "T6_Mbe1_load_P_2min_eql_C3",
"T6_Mbf1_load_P_2min_eql_C1", "T6_Mbf1_load_P_2min_eql_C3",
```

"T5_Pwsnac_2min_avg", "T5_Pwsnac_2min_std",
"T5_PEpow_2min_avg",
"T5_Pnacdrtn_2min_avg", "T5_Pnacdrtn_2min_std",
"T5_Popmode_2min_min", "T5_Popmode_2min_max",
"T5_Ppitch1_2min_min", "T5_Ppitch1_2min_max", "T5_Ppitch1_2min_avg",
"T5_Rspd_2min_avg", "T5_Rspd_2min_std",
"T5_Rspd_2min_min", "T5_Rspd_2min_max",

"T7_Pwsnac_2min_avg", "T7_Pwsnac_2min_std",
"T7_PEpow_2min_avg",
"T7_Pnacdrtn_2min_avg", "T7_Pnacdrtn_2min_std",
"T7_Popmode_2min_min", "T7_Popmode_2min_max",
"T7_Ppitch1_2min_min", "T7_Ppitch1_2min_max", "T7_Ppitch1_2min_avg",
"T7_Rspd_2min_avg", "T7_Rspd_2min_std",
"T7_Rspd_2min_min", "T7_Rspd_2min_max",

"T8_Pwsnac_2min_avg", "T8_Pwsnac_2min_std",
"T8_PEpow_2min_avg",
"T8_Pnacdrtn_2min_avg", "T8_Pnacdrtn_2min_std",
"T8_Popmode_2min_min", "T8_Popmode_2min_max",
"T8_Ppitch1_2min_min", "T8_Ppitch1_2min_max", "T8_Ppitch1_2min_avg",
"T8_Rspd_2min_avg", "T8_Rspd_2min_std",
"T8_Rspd_2min_min", "T8_Rspd_2min_max",

"T9_Pwsnac_2min_avg", "T9_Pwsnac_2min_std",
"T9_PEpow_2min_avg",
"T9_Pnacdrtn_2min_avg", "T9_Pnacdrtn_2min_std",
"T9_Popmode_2min_min", "T9_Popmode_2min_max",
"T9_Ppitch1_2min_min", "T9_Ppitch1_2min_max", "T9_Ppitch1_2min_avg",
"T9_Rspd_2min_avg", "T9_Rspd_2min_std",
"T9_Rspd_2min_min", "T9_Rspd_2min_max"

from (select "t_0",
"MM3_WS80_240_2min_avg", "MM3_WS80_240_2min_std",
"MM3_WS80_240_2min_min", "MM3_WS80_240_2min_max",
"MM3_WD80_240_2min_avg", "MM3_WD80_240_2min_std",
"MM3_WD80_240_2min_min", "MM3_WD80_240_2min_max",
"MM3_Pair80_2min_avg",
"MM3_Tair80_2min_avg",

"T6_Pwsnac_2min_avg", "T6_Pwsnac_2min_std",

"T6_PEpow_2min_avg",
"T6_Pnacdrtn_2min_avg", "T6_Pnacdrtn_2min_std",
"T6_Popmode_2min_min", "T6_Popmode_2min_max",
"T6_Ppitch1_2min_min", "T6_Ppitch1_2min_max", "T6_Ppitch1_2min_avg",
"T6_Rspd_2min_avg", "T6_Rspd_2min_std",
"T6_Rspd_2min_min", "T6_Rspd_2min_max",
"MM3_WS80_true_2min_avg", "MM3_WS80_true_2min_std", "MM3_WS52_true_2min_avg",

"T5_Pwsnac_2min_avg", "T5_Pwsnac_2min_std",
"T5_PEpow_2min_avg",
"T5_Pnacdrtn_2min_avg", "T5_Pnacdrtn_2min_std",
"T5_Popmode_2min_min", "T5_Popmode_2min_max",
"T5_Ppitch1_2min_min", "T5_Ppitch1_2min_max", "T5_Ppitch1_2min_avg",
"T5_Rspd_2min_avg", "T5_Rspd_2min_std",
"T5_Rspd_2min_min", "T5_Rspd_2min_max",

"T7_Pwsnac_2min_avg", "T7_Pwsnac_2min_std",
"T7_PEpow_2min_avg",
"T7_Pnacdrtn_2min_avg", "T7_Pnacdrtn_2min_std",
"T7_Popmode_2min_min", "T7_Popmode_2min_max",
"T7_Ppitch1_2min_min", "T7_Ppitch1_2min_max", "T7_Ppitch1_2min_avg",
"T7_Rspd_2min_avg", "T7_Rspd_2min_std",
"T7_Rspd_2min_min", "T7_Rspd_2min_max",

"T8_Pwsnac_2min_avg", "T8_Pwsnac_2min_std",
"T8_PEpow_2min_avg",
"T8_Pnacdrtn_2min_avg", "T8_Pnacdrtn_2min_std",
"T8_Popmode_2min_min", "T8_Popmode_2min_max",
"T8_Ppitch1_2min_min", "T8_Ppitch1_2min_max", "T8_Ppitch1_2min_avg",
"T8_Rspd_2min_avg", "T8_Rspd_2min_std",
"T8_Rspd_2min_min", "T8_Rspd_2min_max",

"T9_Pwsnac_2min_avg", "T9_Pwsnac_2min_std",
"T9_PEpow_2min_avg",
"T9_Pnacdrtn_2min_avg", "T9_Pnacdrtn_2min_std",
"T9_Popmode_2min_min", "T9_Popmode_2min_max",
"T9_Ppitch1_2min_min", "T9_Ppitch1_2min_max", "T9_Ppitch1_2min_avg",
"T9_Rspd_2min_avg", "T9_Rspd_2min_std",
"T9_Rspd_2min_min", "T9_Rspd_2min_max"

from public."statistics_2m"

```

where
"MM3_WD80_240_2min_avg">200 and "MM3_WD80_240_2min_avg"<300 and
"T6_Popmode_2min_min">10.5 and "T6_Popmode_2min_max"<14.5 and
"T5_Popmode_2min_min">10.5 and "T5_Popmode_2min_max"<14.5 and
"T7_Popmode_2min_min">10.5 and "T7_Popmode_2min_max"<14.5 and
"T8_Popmode_2min_min">10.5 and "T8_Popmode_2min_max"<14.5 and
"T9_Popmode_2min_min">10.5 and "T9_Popmode_2min_max"<14.5 and
"T6_PEpow_2min_avg">25 and "T5_PEpow_2min_avg">25 and "T7_PEpow_2min_avg">25 and "T8_PEpow_2m
) as "r1" join
(
select
    "t_0",
    "T6_Mbe1_load_P_2min_eql_C1", "T6_Mbf1_load_P_2min_eql_C1",
    "T6_Mbe1_load_P_2min_eql_C3", "T6_Mbf1_load_P_2min_eql_C3"
from public.eq1_2m
) as "r2"
on (r1.t_0 = r2.t_0)
order by r1."t_0"

/*

"T6_Pwsnac_2min_std",
"T5_Pwsnac_2min_avg",

"T5_PEpow_2min_avg",
"T5_Pnacdrtn_2min_avg", "T5_Pnacdrtn_2min_std",
"T5_Popmode_2min_min", "T5_Popmode_2min_max",
"T5_Ppitch1_2min_min", "T5_Ppitch1_2min_max",
"T5_Rspd_2min_avg", "T5_Rspd_2min_std",

*/

```

A.2 Loads (T5-6)

SQL script for 2 minute average data

```
select r1."t_0",
"MM3_WS80_240_2min_avg","MM3_WS80_240_2min_std",
"MM3_WD80_240_2min_avg","MM3_WD80_240_2min_std",
"MM3_Pair80_2min_avg",
"MM3_Tair80_2min_avg",

"T6_Pwsnac_2min_avg",
"T6_PEpow_2min_avg",
"T6_Pnacdrtn_2min_avg","T6_Pnacdrtn_2min_std",
"T6_Popmode_2min_min","T6_Popmode_2min_max",
"T6_Ppitch1_2min_min","T6_Ppitch1_2min_max",
"T6_Rspd_2min_avg","T6_Rspd_2min_std",
"MM3_WS80_true_2min_avg", "MM3_WS80_true_2min_std", "MM3_WS52_true_2min_avg",

r2."t_0",
"T6_Mbe1_load_P_2min_eql_C1","T6_Mbe1_load_P_2min_eql_C3",
"T6_Mbf1_load_P_2min_eql_C1","T6_Mbf1_load_P_2min_eql_C3",

"T5_Pwsnac_2min_avg",
"T5_PEpow_2min_avg",
"T5_Pnacdrtn_2min_avg", "T5_Pnacdrtn_2min_std",
"T5_Popmode_2min_min", "T5_Popmode_2min_max",
"T5_Ppitch1_2min_min", "T5_Ppitch1_2min_max",
"T5_Rspd_2min_avg", "T5_Rspd_2min_std",

"T5_Pwsnac_2min_std",
"T6_Pwsnac_2min_std"

from ( select "t_0", "MM3_WS80_240_2min_avg","MM3_WS80_240_2min_std",
"MM3_WD80_240_2min_avg","MM3_WD80_240_2min_std",
"MM3_Pair80_2min_avg",
"MM3_Tair80_2min_avg",
"T6_Pwsnac_2min_avg",

"T6_PEpow_2min_avg",
"T6_Pnacdrtn_2min_avg","T6_Pnacdrtn_2min_std",
"T6_Popmode_2min_min","T6_Popmode_2min_max",
"T6_Ppitch1_2min_min","T6_Ppitch1_2min_max",
```

```

"T6_Rspd_2min_avg", "T6_Rspd_2min_std",
"MM3_WS80_true_2min_avg", "MM3_WS80_true_2min_std",
"MM3_WS52_true_2min_avg",

"T5_Pwsnac_2min_avg",
"T5_PEpow_2min_avg",
"T5_Pnacdrtn_2min_avg", "T5_Pnacdrtn_2min_std",
"T5_Popmode_2min_min", "T5_Popmode_2min_max",
"T5_Ppitch1_2min_min", "T5_Ppitch1_2min_max",
"T5_Rspd_2min_avg", "T5_Rspd_2min_std",

"T5_Pwsnac_2min_std",
"T6_Pwsnac_2min_std"

from public."statistics_2m"
where
"MM3_WD80_240_2min_avg">200 and "MM3_WD80_240_2min_avg"<300 and
"T6_Popmode_2min_min">10.5 and "T6_Popmode_2min_max"<14.5 and
"T6_PEpow_2min_avg">25
) as "r1" join
(
select
  "t_0",
  "T6_Mbe1_load_P_2min_eql_C1", "T6_Mbf1_load_P_2min_eql_C1",
  "T6_Mbe1_load_P_2min_eql_C3", "T6_Mbf1_load_P_2min_eql_C3"
from public.eql_2m
) as "r2"
on (r1.t_0 = r2.t_0)
order by r1."t_0"

/*

"T6_Pwsnac_2min_std",
"T5_Pwsnac_2min_avg",

"T5_PEpow_2min_avg",
"T5_Pnacdrtn_2min_avg", "T5_Pnacdrtn_2min_std",
"T5_Popmode_2min_min", "T5_Popmode_2min_max",
"T5_Ppitch1_2min_min", "T5_Ppitch1_2min_max",
"T5_Rspd_2min_avg", "T5_Rspd_2min_std",

```

*/

B

Data reduction logs

B.1 Power (T5-9)

————— Data reduction log for 00000 (2 minute average) —————

```
"start length:281138"  
"NaN in yaw_T5:4070"  
"NaN in yaw_T6:4170"  
"NaN in yaw_T7:2740"  
"NaN in yaw_T8:2027"  
"NaN in yaw_T9:646"  
"NA in Pair:3881"  
"power T5>25:0"  
"power T6>25:0"  
"power T7>25:0"  
"power T8>25:0"  
"power T9>25:0"  
"nacelle dir std T5 (<15) :1"  
"nacelle dir std T6 (<15) :0"  
"nacelle dir std T7 (<15) :1"  
"nacelle dir std T8 (<15) :2"  
"nacelle dir std T9 (<15) :0"  
"windspeed (5 to 15 m/s) :29720"  
"v/v_nac T5 (0.85 to 1.15) :24979"  
"v/v_nac T5 (>0.85) :0"
```

"v/v_nac T6 (>0.85) :2723"
"v/v_nac T7 (>0.85) :1874"
"v/v_nac T8 (>0.85) :5329"
"v/v_nac T9 (>0.85) :912"
"TI (0.01 to 0.2) :1376"
"pitch_dif T5 (<0.2 deg) :25356"
"pitch_dif T6 (<0.2 deg) :2627"
"pitch_dif T7 (<0.2 deg) :823"
"pitch_dif T8 (<0.2 deg) :1953"
"pitch_dif T9 (<0.2 deg) :1464"
"wind shear ws80/ws50 (1 to 1.2):32067"
"Misalignment T5 (-20 to 12.5):1582"
"Misalignment T6 (-20 to 12.5):317"
"Misalignment T7 (-20 to 12.5):432"
"Misalignment T8 (-20 to 12.5):7077"
"Misalignment T9 (-20 to 12.5):1103"
"pitch_angle T5 - T9 (0 / 0 / 0.2 / 0 / 0 deg, bandwidth +/-0.2) :17691"
"final length:104195"

_____ Data reduction log for 20000 (2 minute average) _____

"start length:281138"
"NaN in yaw_T5:4070"
"NaN in yaw_T6:4170"
"NaN in yaw_T7:2740"
"NaN in yaw_T8:2027"
"NaN in yaw_T9:646"
"NA in Pair:3881"
"power T5>25:0"
"power T6>25:0"
"power T7>25:0"
"power T8>25:0"
"power T9>25:0"
"nacelle dir std T5 (<15) :1"
"nacelle dir std T6 (<15) :0"
"nacelle dir std T7 (<15) :1"
"nacelle dir std T8 (<15) :2"
"nacelle dir std T9 (<15) :0"
"windspeed (5 to 15 m/s) :29720"

"v/v_nac T5 (0.85 to 1.15) :24979"
"v/v_nac T5 (>0.85) :0"
"v/v_nac T6 (>0.85) :2723"
"v/v_nac T7 (>0.85) :1874"
"v/v_nac T8 (>0.85) :5329"
"v/v_nac T9 (>0.85) :912"
"TI (0.01 to 0.2) :1376"
"pitch_dif T5 (<0.2 deg) :25356"
"pitch_dif T6 (<0.2 deg) :2627"
"pitch_dif T7 (<0.2 deg) :823"
"pitch_dif T8 (<0.2 deg) :1953"
"pitch_dif T9 (<0.2 deg) :1464"
"wind shear ws80/ws50 (1 to 1.2):32067"
"Misalignment T5 (-20 to 12.5):1582"
"Misalignment T6 (-20 to 12.5):317"
"Misalignment T7 (-20 to 12.5):432"
"Misalignment T8 (-20 to 12.5):7077"
"Misalignment T9 (-20 to 12.5):1103"
"pitch_angle T5 - T9 (2 / 0 / 0.2 / 0 / 0 deg, bandwidth +/-0.2) :116584"
"final length:5302"

_____ Data reduction log for 40000 (2 minute average) _____

"start length:281138"
"NaN in yaw_T5:4070"
"NaN in yaw_T6:4170"
"NaN in yaw_T7:2740"
"NaN in yaw_T8:2027"
"NaN in yaw_T9:646"
"NA in Pair:3881"
"power T5>25:0"
"power T6>25:0"
"power T7>25:0"
"power T8>25:0"
"power T9>25:0"
"nacelle dir std T5 (<15) :1"
"nacelle dir std T6 (<15) :0"
"nacelle dir std T7 (<15) :1"
"nacelle dir std T8 (<15) :2"

"nacelle dir std T9 (<15) :0"
"windspeed (5 to 15 m/s) :29720"
"v/v_nac T5 (0.85 to 1.15) :24979"
"v/v_nac T5 (>0.85) :0"
"v/v_nac T6 (>0.85) :2723"
"v/v_nac T7 (>0.85) :1874"
"v/v_nac T8 (>0.85) :5329"
"v/v_nac T9 (>0.85) :912"
"TI (0.01 to 0.2) :1376"
"pitch_dif T5 (<0.2 deg) :25356"
"pitch_dif T6 (<0.2 deg) :2627"
"pitch_dif T7 (<0.2 deg) :823"
"pitch_dif T8 (<0.2 deg) :1953"
"pitch_dif T9 (<0.2 deg) :1464"
"wind shear ws80/ws50 (1 to 1.2):32067"
"Misalignment T5 (-20 to 12.5):1582"
"Misalignment T6 (-20 to 12.5):317"
"Misalignment T7 (-20 to 12.5):432"
"Misalignment T8 (-20 to 12.5):7077"
"Misalignment T9 (-20 to 12.5):1103"
"pitch_angle T5 - T9 (4 / 0 / 0.2 / 0 / 0 deg, bandwidth +/-0.2) :121886"
"final length:0"

B.2 Loads (T5-6)

----- Data reduction log for 00xxx (2 minute average) -----

```
"start length:595277"  
"NaN in yaw_T6:4785"  
"NaN in yaw_T5:34978"  
"NA in Pair:6392"  
"NA in Medge_C1:166145"  
"NA in Mflat_C1:0"  
"NA in Medge_C2:0"  
"NA in Mflat_C2:0"  
"power T6>25:0"  
"power T5>25:29554"  
"nacelle dir std T6 (<15) :1"  
"nacelle dir std T5 (<15) :4"  
"windspeed (5 to 15 m/s) :47348"  
"v/v_nac T5 (0.85 to 1.15) :33038"  
"TI (0.01 to 0.2) :1891"  
"pitch_dif T6 (<0.2 deg) :33282"  
"pitch_dif T5 (<0.2 deg) :8170"  
"wind shear ws80/ws50 (1 to 1.2 ):43853"  
"Misalignment T6 (-12.5 to 2.5 ):17930"  
"Misalignment T5 (-12.5 to 2.5 ):29777"  
"pitch_angle T5 / T6 (0 / 0 deg, bandwidth +/-0.2) :10272"  
"final length:127857"
```

----- Data reduction log for 00xxx (5 minute average) -----

```
"start length:228179"  
"NaN in yaw_T6:1913"  
"NaN in yaw_T5:25755"  
"NA in Pair:1998"  
"NA in Medge_C1:43149"  
"NA in Mflat_C1:0"  
"NA in Medge_C2:0"  
"NA in Mflat_C2:0"  
"power T6>25:0"
```

"power T5>25:11632"
"nacelle dir std T6 (<15) :18"
"nacelle dir std T5 (<15) :12"
"windspeed (5 to 15 m/s) :18730"
"v/v_nac T5 (0.85 to 1.15) :7093"
"TI (0.01 to 0.2) :331"
"pitch_dif T6 (<0.2 deg) :17266"
"pitch_dif T5 (<0.2 deg) :3550"
"wind shear ws80/ws50 (1 to 1.2):15513"
"Misalignment T6 (-12.5 to 2.5):5898"
"Misalignment T5 (-12.5 to 2.5):11957"
"pitch_angle T5 / T6 (0 / 0 deg, bandwidth +/-0.2) :5762"
"final length:57602"

_____ Data reduction log for 00xxx (10 minute average) _____

"start length:89013"
"NaN in yaw_T6:893"
"NaN in yaw_T5:1350"
"NA in Pair:986"
"NA in Medge_C1:18285"
"NA in Mflat_C1:0"
"NA in Medge_C2:0"
"NA in Mflat_C2:0"
"power T6>25:0"
"power T5>25:0"
"nacelle dir std T6 (<15) :36"
"nacelle dir std T5 (<15) :11"
"windspeed (5 to 15 m/s) :8530"
"v/v_nac T5 (0.85 to 1.15) :1592"
"TI (0.01 to 0.2) :205"
"pitch_dif T6 (<0.2 deg) :9691"
"pitch_dif T5 (<0.2 deg) :1586"
"wind shear ws80/ws50 (1 to 1.2):7996"
"Misalignment T6 (-12.5 to 2.5):1871"
"Misalignment T5 (-12.5 to 2.5):4742"
"pitch_angle T5 / T6 (0 / 0 deg, bandwidth +/-0.2) :2400"
"final length:28839"

_____ Data reduction log for 20xxx (2 minute average) _____

"start length:595277"
"NaN in yaw_T6:4785"
"NaN in yaw_T5:34978"
"NA in Pair:6392"
"NA in Medge_C1:166145"
"NA in Mflat_C1:0"
"NA in Medge_C2:0"
"NA in Mflat_C2:0"
"power T6>25:0"
"power T5>25:29554"
"nacelle dir std T6 (<15) :1"
"nacelle dir std T5 (<15) :4"
"windspeed (5 to 15 m/s) :47348"
"v/v_nac T5 (0.85 to 1.15) :33038"
"TI (0.01 to 0.2) :1891"
"pitch_dif T6 (<0.2 deg) :33282"
"pitch_dif T5 (<0.2 deg) :8170"
"wind shear ws80/ws50 (1 to 1.2):43853"
"Misalignment T6 (-12.5 to 2.5):17930"
"Misalignment T5 (-12.5 to 2.5):29777"
"pitch_angle T5 / T6 (2 / 0 deg, bandwidth +/-0.2) :132668"
"final length:5461"

_____ Data reduction log for 20xxx (5 minute average) _____

"start length:228179"
"NaN in yaw_T6:1913"
"NaN in yaw_T5:25755"
"NA in Pair:1998"
"NA in Medge_C1:43149"
"NA in Mflat_C1:0"
"NA in Medge_C2:0"
"NA in Mflat_C2:0"
"power T6>25:0"

"power T5>25:11632"
"nacelle dir std T6 (<15) :18"
"nacelle dir std T5 (<15) :12"
"windspeed (5 to 15 m/s) :18730"
"v/v_nac T5 (0.85 to 1.15) :7093"
"TI (0.01 to 0.2) :331"
"pitch_dif T6 (<0.2 deg) :17266"
"pitch_dif T5 (<0.2 deg) :3550"
"wind shear ws80/ws50 (1 to 1.2):15513"
"Misalignment T6 (-12.5 to 2.5):5898"
"Misalignment T5 (-12.5 to 2.5):11957"
"pitch_angle T5 / T6 (2 / 0 deg, bandwidth +/-0.2) :60954"
"final length:2410"

_____ Data reduction log for 20xxx (10 minute average) _____

"start length:89013"
"NaN in yaw_T6:893"
"NaN in yaw_T5:1350"
"NA in Pair:986"
"NA in Medge_C1:18285"
"NA in Mflat_C1:0"
"NA in Medge_C2:0"
"NA in Mflat_C2:0"
"power T6>25:0"
"power T5>25:0"
"nacelle dir std T6 (<15) :36"
"nacelle dir std T5 (<15) :11"
"windspeed (5 to 15 m/s) :8530"
"v/v_nac T5 (0.85 to 1.15) :1592"
"TI (0.01 to 0.2) :205"
"pitch_dif T6 (<0.2 deg) :9691"
"pitch_dif T5 (<0.2 deg) :1586"
"wind shear ws80/ws50 (1 to 1.2):7996"
"Misalignment T6 (-12.5 to 2.5):1871"
"Misalignment T5 (-12.5 to 2.5):4742"
"pitch_angle T5 / T6 (2 / 0 deg, bandwidth +/-0.2) :29954"
"final length:1285"

_____ Data reduction log for 40xxx (2 minute average) _____

"start length:595277"
"NaN in yaw_T6:4785"
"NaN in yaw_T5:34978"
"NA in Pair:6392"
"NA in Medge_C1:166145"
"NA in Mflat_C1:0"
"NA in Medge_C2:0"
"NA in Mflat_C2:0"
"power T6>25:0"
"power T5>25:29554"
"nacelle dir std T6 (<15) :1"
"nacelle dir std T5 (<15) :4"
"windspeed (5 to 15 m/s) :47348"
"v/v_nac T5 (0.85 to 1.15) :33038"
"TI (0.01 to 0.2) :1891"
"pitch_dif T6 (<0.2 deg) :33282"
"pitch_dif T5 (<0.2 deg) :8170"
"wind shear ws80/ws50 (1 to 1.2):43853"
"Misalignment T6 (-12.5 to 2.5):17930"
"Misalignment T5 (-12.5 to 2.5):29777"
"pitch_angle T5 / T6 (4 / 0 deg, bandwidth +/-0.2) :136340"
"final length:1789"

_____ Data reduction log for 40xxx (5 minute average) _____

"start length:228179"
"NaN in yaw_T6:1913"
"NaN in yaw_T5:25755"
"NA in Pair:1998"
"NA in Medge_C1:43149"
"NA in Mflat_C1:0"
"NA in Medge_C2:0"
"NA in Mflat_C2:0"
"power T6>25:0"

"power T5>25:11632"
"nacelle dir std T6 (<15) :18"
"nacelle dir std T5 (<15) :12"
"windspeed (5 to 15 m/s) :18730"
"v/v_nac T5 (0.85 to 1.15) :7093"
"TI (0.01 to 0.2) :331"
"pitch_dif T6 (<0.2 deg) :17266"
"pitch_dif T5 (<0.2 deg) :3550"
"wind shear ws80/ws50 (1 to 1.2):15513"
"Misalignment T6 (-12.5 to 2.5):5898"
"Misalignment T5 (-12.5 to 2.5):11957"
"pitch_angle T5 / T6 (4 / 0 deg, bandwidth +/-0.2) :62467"
"final length:897"

_____ Data reduction log for 40xxx (10 minute average) _____

"start length:89013"
"NaN in yaw_T6:893"
"NaN in yaw_T5:1350"
"NA in Pair:986"
"NA in Medge_C1:18285"
"NA in Mflat_C1:0"
"NA in Medge_C2:0"
"NA in Mflat_C2:0"
"power T6>25:0"
"power T5>25:0"
"nacelle dir std T6 (<15) :36"
"nacelle dir std T5 (<15) :11"
"windspeed (5 to 15 m/s) :8530"
"v/v_nac T5 (0.85 to 1.15) :1592"
"TI (0.01 to 0.2) :205"
"pitch_dif T6 (<0.2 deg) :9691"
"pitch_dif T5 (<0.2 deg) :1586"
"wind shear ws80/ws50 (1 to 1.2):7996"
"Misalignment T6 (-12.5 to 2.5):1871"
"Misalignment T5 (-12.5 to 2.5):4742"
"pitch_angle T5 / T6 (4 / 0 deg, bandwidth +/-0.2) :30797"
"final length:442"

_____ Data reduction log for 22xxx (2 minute average) _____

"start length:595277"
"NaN in yaw_T6:4785"
"NaN in yaw_T5:34978"
"NA in Pair:6392"
"NA in Medge_C1:166145"
"NA in Mflat_C1:0"
"NA in Medge_C2:0"
"NA in Mflat_C2:0"
"power T6>25:0"
"power T5>25:29554"
"nacelle dir std T6 (<15) :1"
"nacelle dir std T5 (<15) :4"
"windspeed (5 to 15 m/s) :47348"
"v/v_nac T5 (0.85 to 1.15) :33038"
"TI (0.01 to 0.2) :1891"
"pitch_dif T6 (<0.2 deg) :33282"
"pitch_dif T5 (<0.2 deg) :8170"
"wind shear ws80/ws50 (1 to 1.2):43853"
"Misalignment T6 (-12.5 to 2.5):17930"
"Misalignment T5 (-12.5 to 2.5):29777"
"pitch_angle T5 / T6 (2 / 2 deg, bandwidth +/-0.2) :136512"
"final length:1617"

_____ Data reduction log for 22xxx (5 minute average) _____

"start length:228179"
"NaN in yaw_T6:1913"
"NaN in yaw_T5:25755"
"NA in Pair:1998"
"NA in Medge_C1:43149"
"NA in Mflat_C1:0"
"NA in Medge_C2:0"
"NA in Mflat_C2:0"
"power T6>25:0"

"power T5>25:11632"
"nacelle dir std T6 (<15) :18"
"nacelle dir std T5 (<15) :12"
"windspeed (5 to 15 m/s) :18730"
"v/v_nac T5 (0.85 to 1.15) :7093"
"TI (0.01 to 0.2) :331"
"pitch_dif T6 (<0.2 deg) :17266"
"pitch_dif T5 (<0.2 deg) :3550"
"wind shear ws80/ws50 (1 to 1.2):15513"
"Misalignment T6 (-12.5 to 2.5):5898"
"Misalignment T5 (-12.5 to 2.5):11957"
"pitch_angle T5 / T6 (2 / 2 deg, bandwidth +/-0.2) :62633"
"final length:731"

_____ Data reduction log for 22xxx (10 minute average) _____

"start length:89013"
"NaN in yaw_T6:893"
"NaN in yaw_T5:1350"
"NA in Pair:986"
"NA in Medge_C1:18285"
"NA in Mflat_C1:0"
"NA in Medge_C2:0"
"NA in Mflat_C2:0"
"power T6>25:0"
"power T5>25:0"
"nacelle dir std T6 (<15) :36"
"nacelle dir std T5 (<15) :11"
"windspeed (5 to 15 m/s) :8530"
"v/v_nac T5 (0.85 to 1.15) :1592"
"TI (0.01 to 0.2) :205"
"pitch_dif T6 (<0.2 deg) :9691"
"pitch_dif T5 (<0.2 deg) :1586"
"wind shear ws80/ws50 (1 to 1.2):7996"
"Misalignment T6 (-12.5 to 2.5):1871"
"Misalignment T5 (-12.5 to 2.5):4742"
"pitch_angle T5 / T6 (2 / 2 deg, bandwidth +/-0.2) :30837"
"final length:402"

C

Data reduction figures

C.1 Power (T5-9)

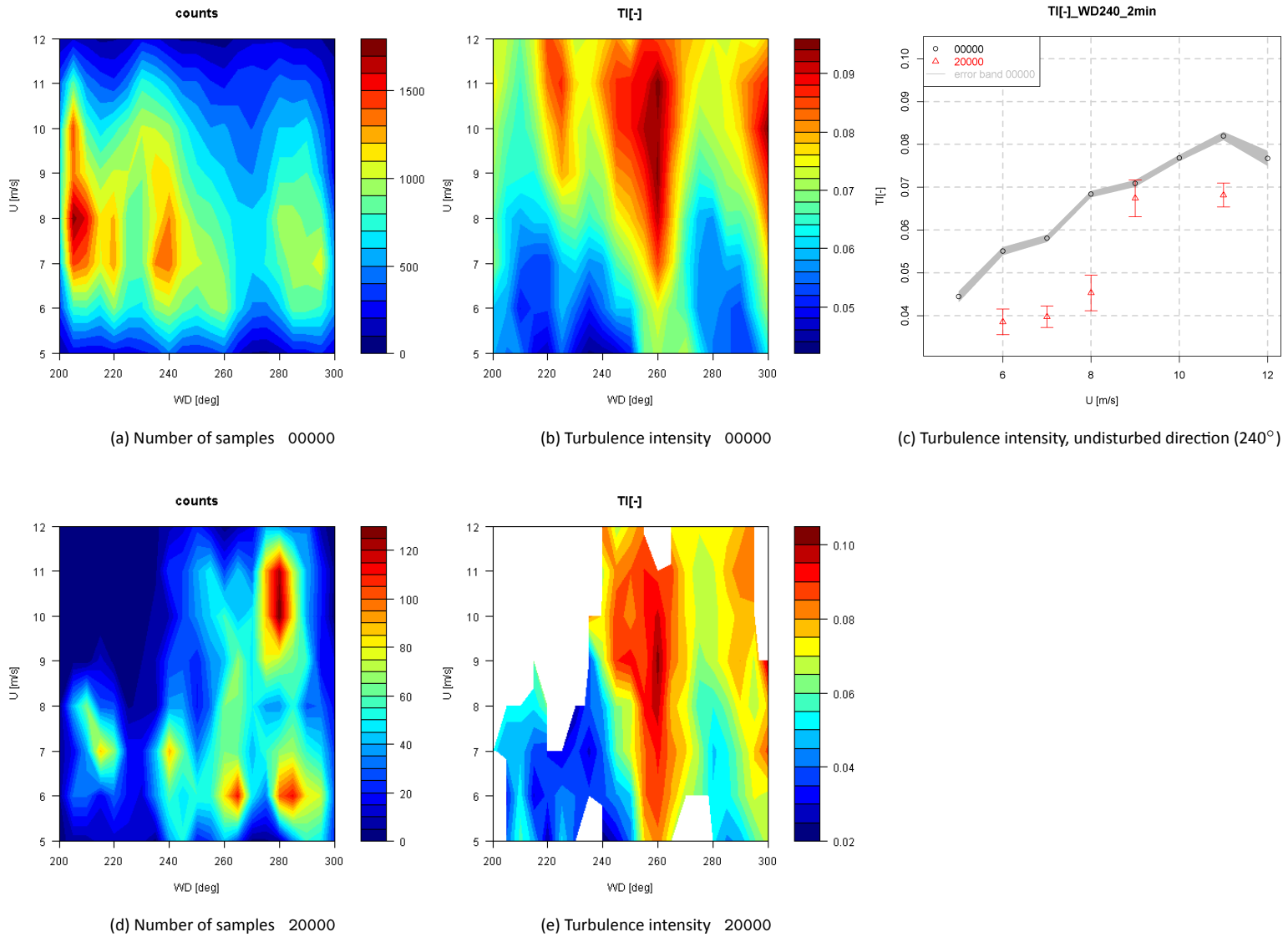
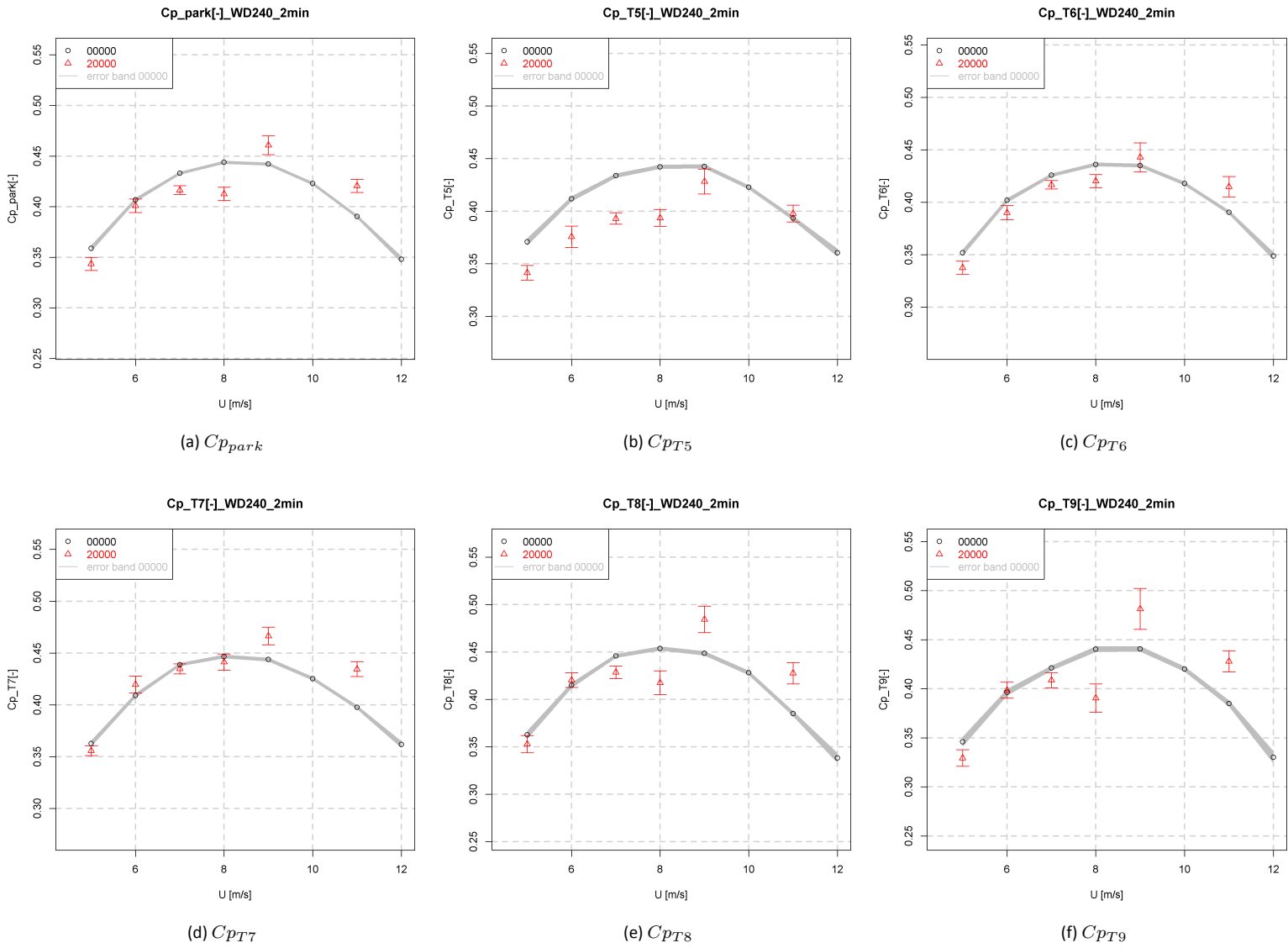


Figure 14: Number of samples and turbulence intensity for configuration 00000 and 20000 (2 minute average)


 Figure 15: Variation of C_p with wind speed for undisturbed wind direction (240°), 2 minute average

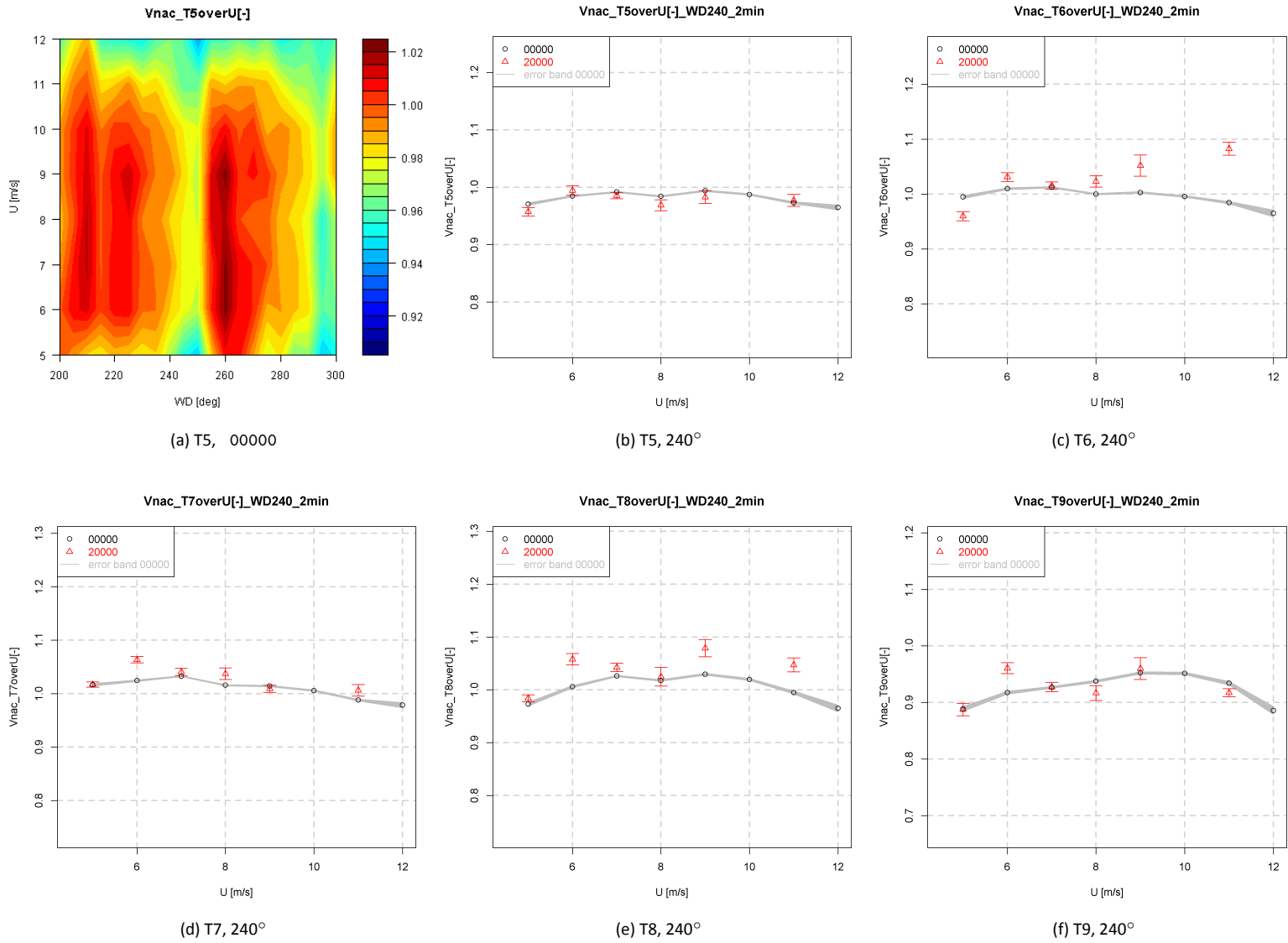
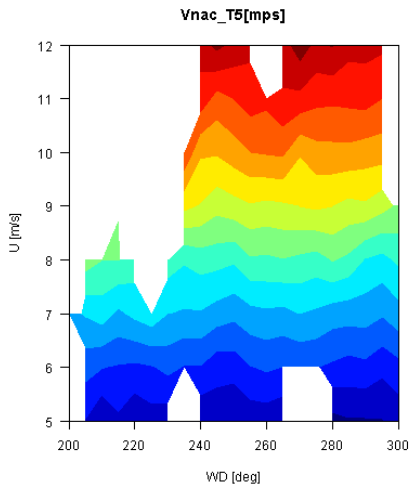
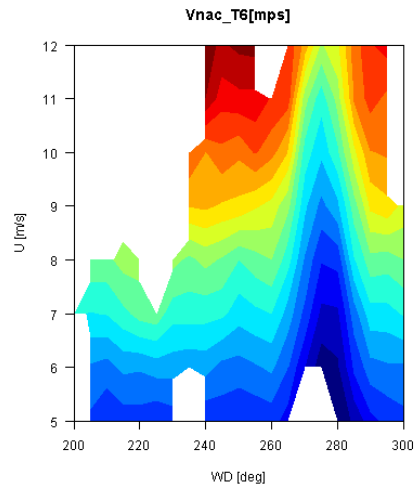


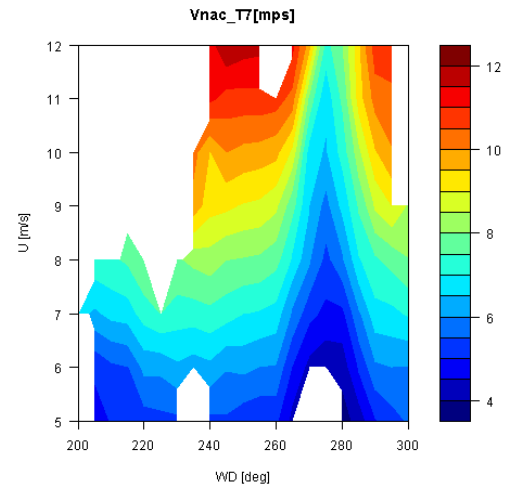
Figure 16: Variation of nacelle wind speed over meteo mast wind speed ratio with wind speed, undisturbed sector, 2 minute average



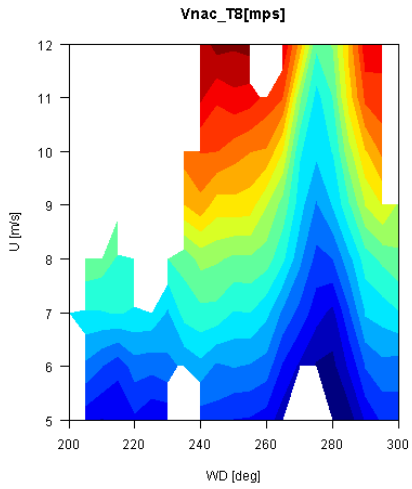
(a) Nacelle wind speed of turbine 5



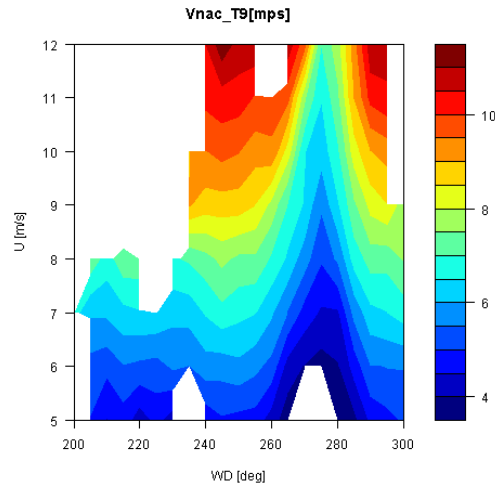
(b) Nacelle wind speed of turbine 6



(c) Nacelle wind speed of turbine 7



(d) Nacelle wind speed of turbine 8



(e) Nacelle wind speed of turbine 9

Figure 17: Nacelle wind speed of turbine 5 to 9 for configuration 00000, 2 minute average

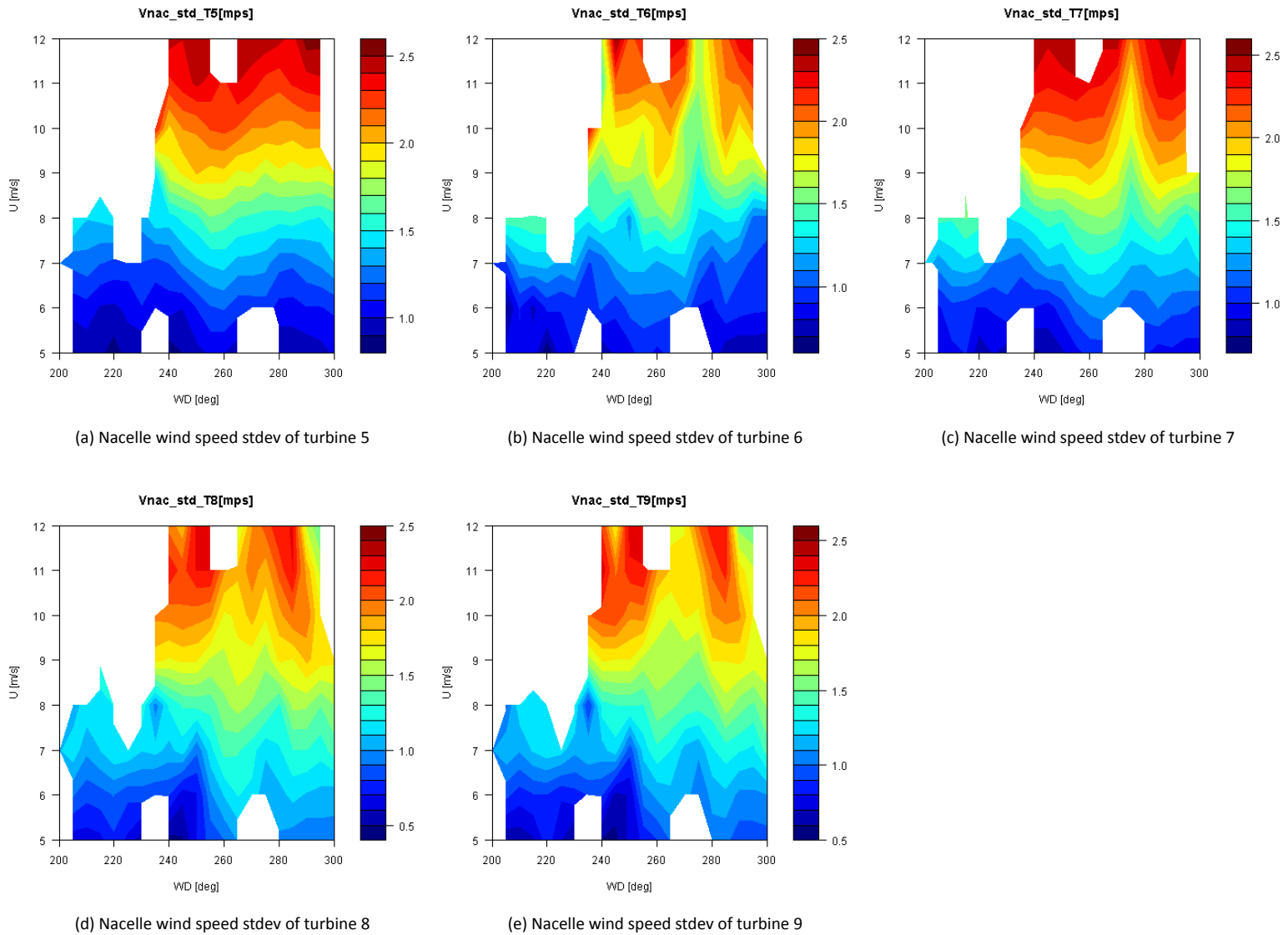
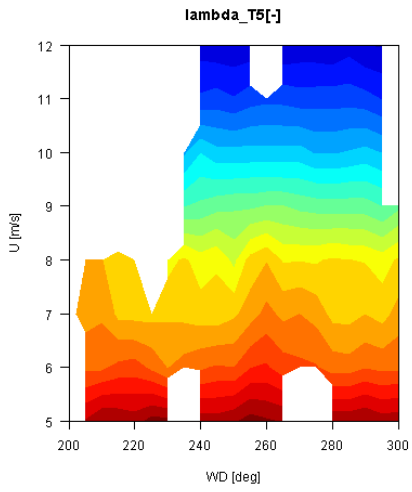
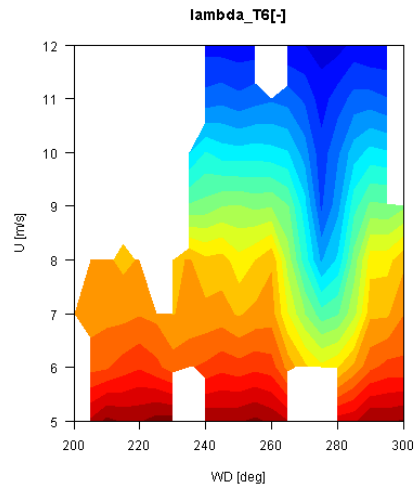


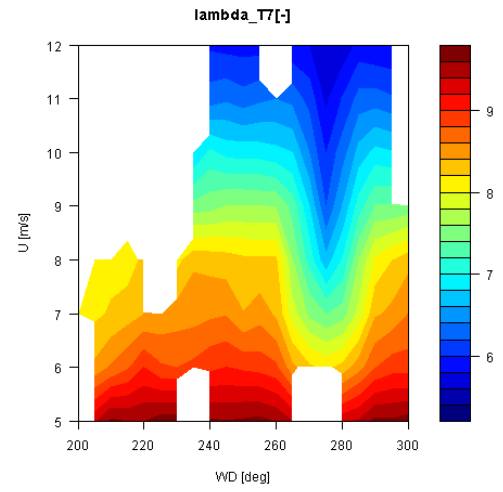
Figure 18: Nacelle wind speed standard deviation of turbine 5 to 9 for configuration 00000, 2 minute average



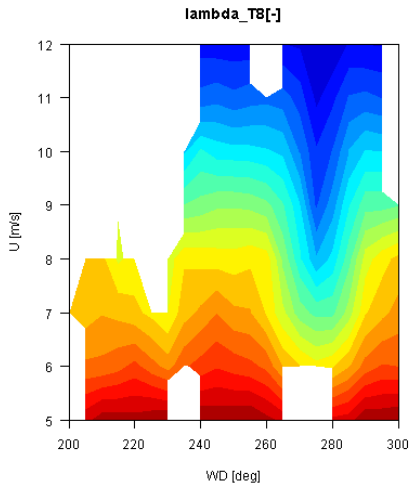
(a) Tip speed ratio of turbine 5



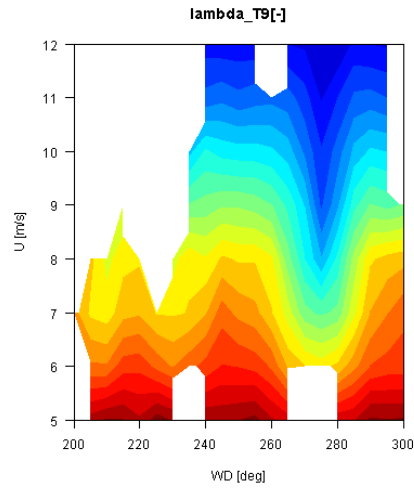
(b) Tip speed ratio of turbine 6



(c) Tip speed ratio of turbine 7



(d) Tip speed ratio of turbine 8



(e) Tip speed ratio of turbine 9

Figure 19: Tip speed ratio of turbine 5 to 9 for configuration 00000, 2 minute average

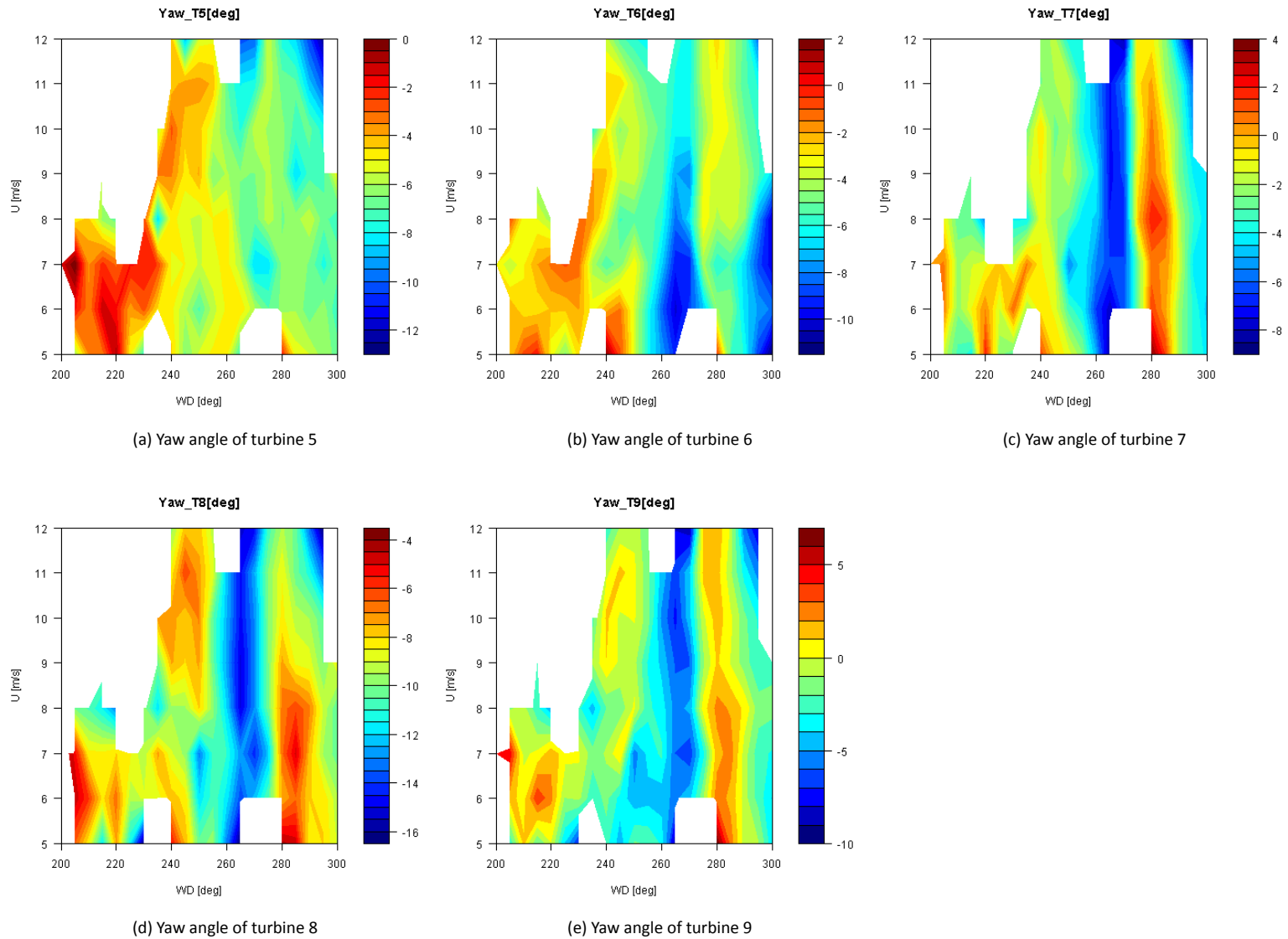


Figure 20: Yaw angle of turbine 5 to 9 for configuration 00000, 2 minute average

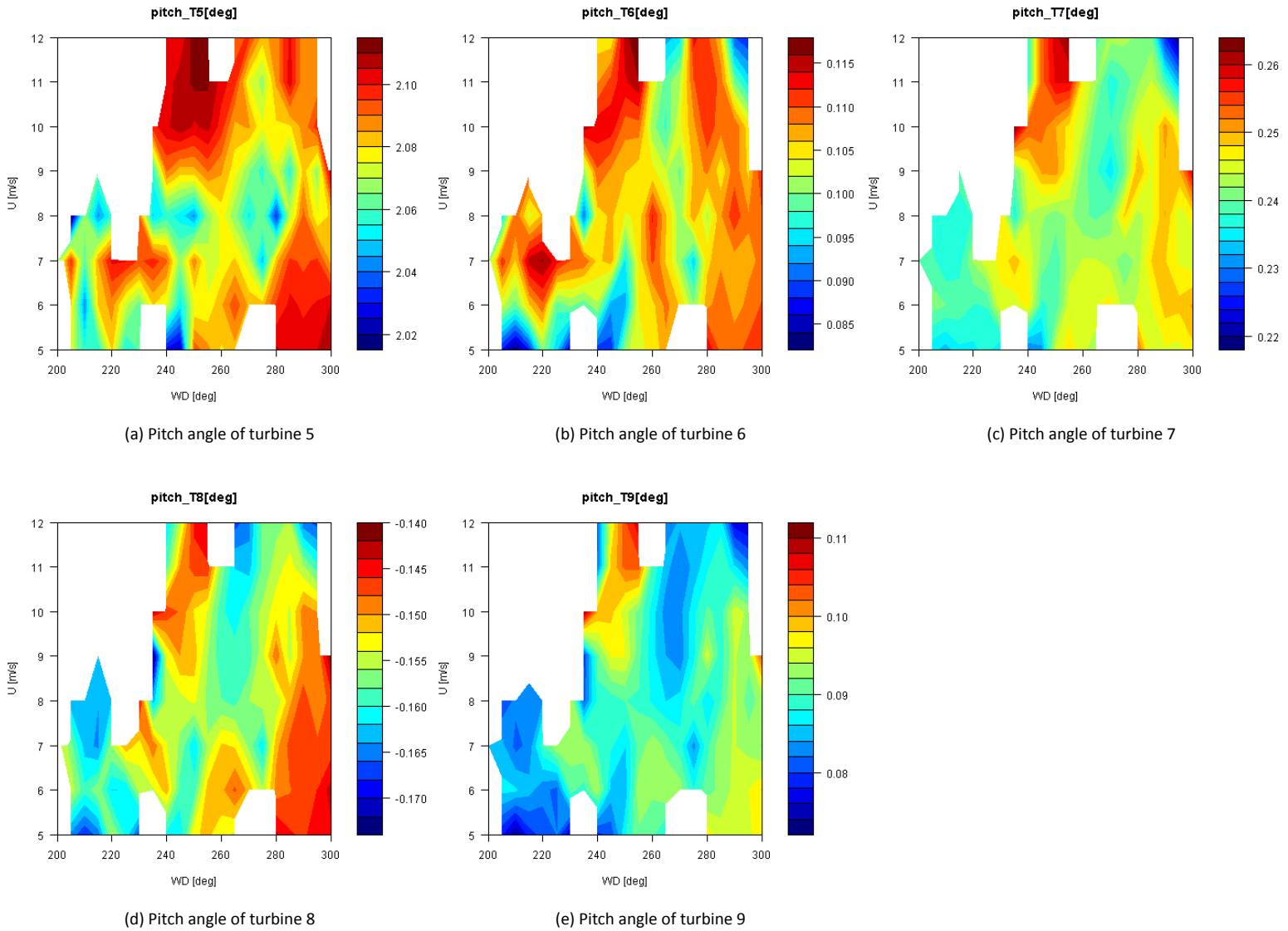


Figure 21: Pitch angle of turbine 5 to 9 for configuration 00000, 2 minute average

C.2 Loads (T5-6)

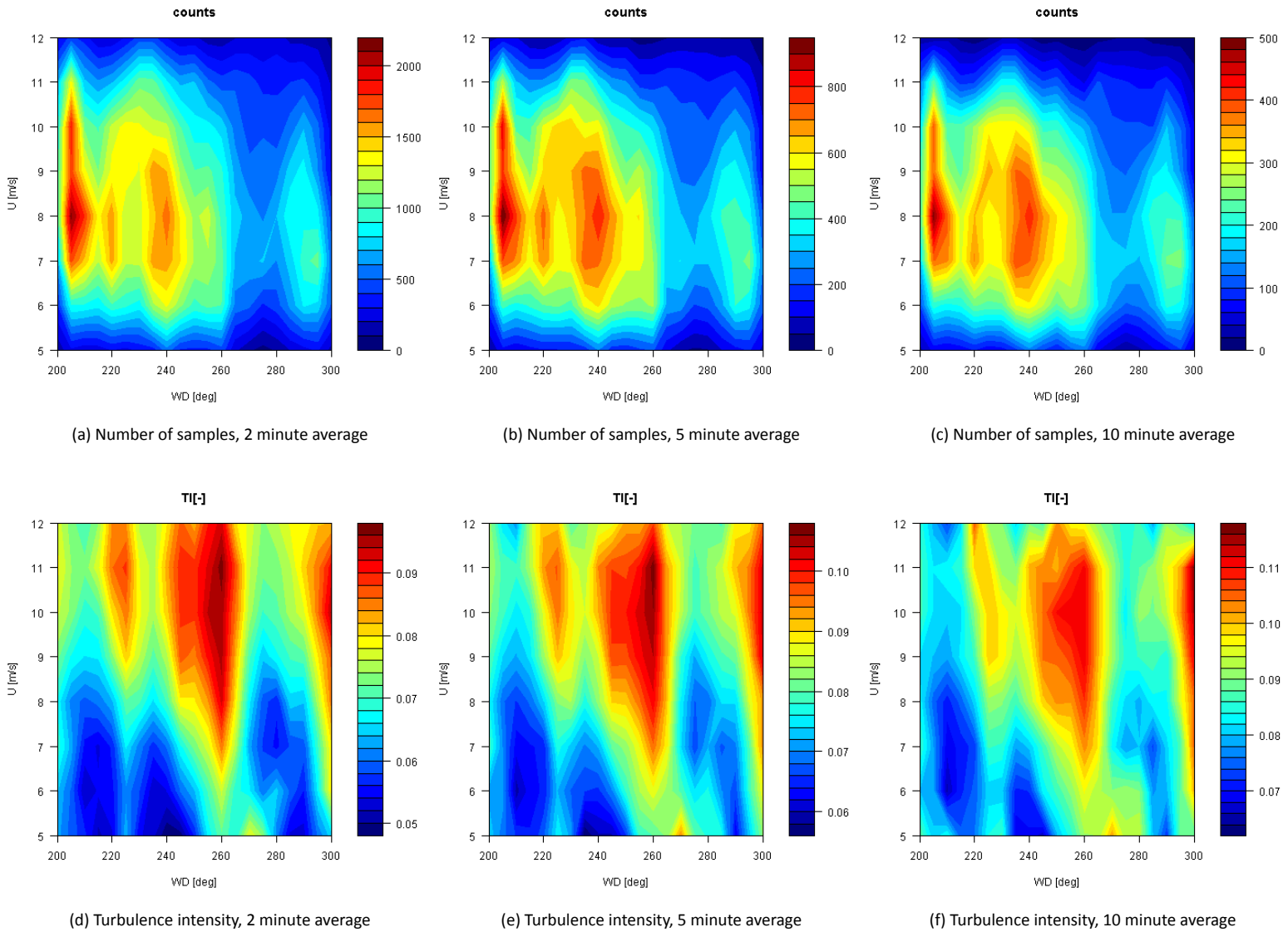


Figure 22: Number of samples (above) and turbulence intensity (below) for configuration 00xxx

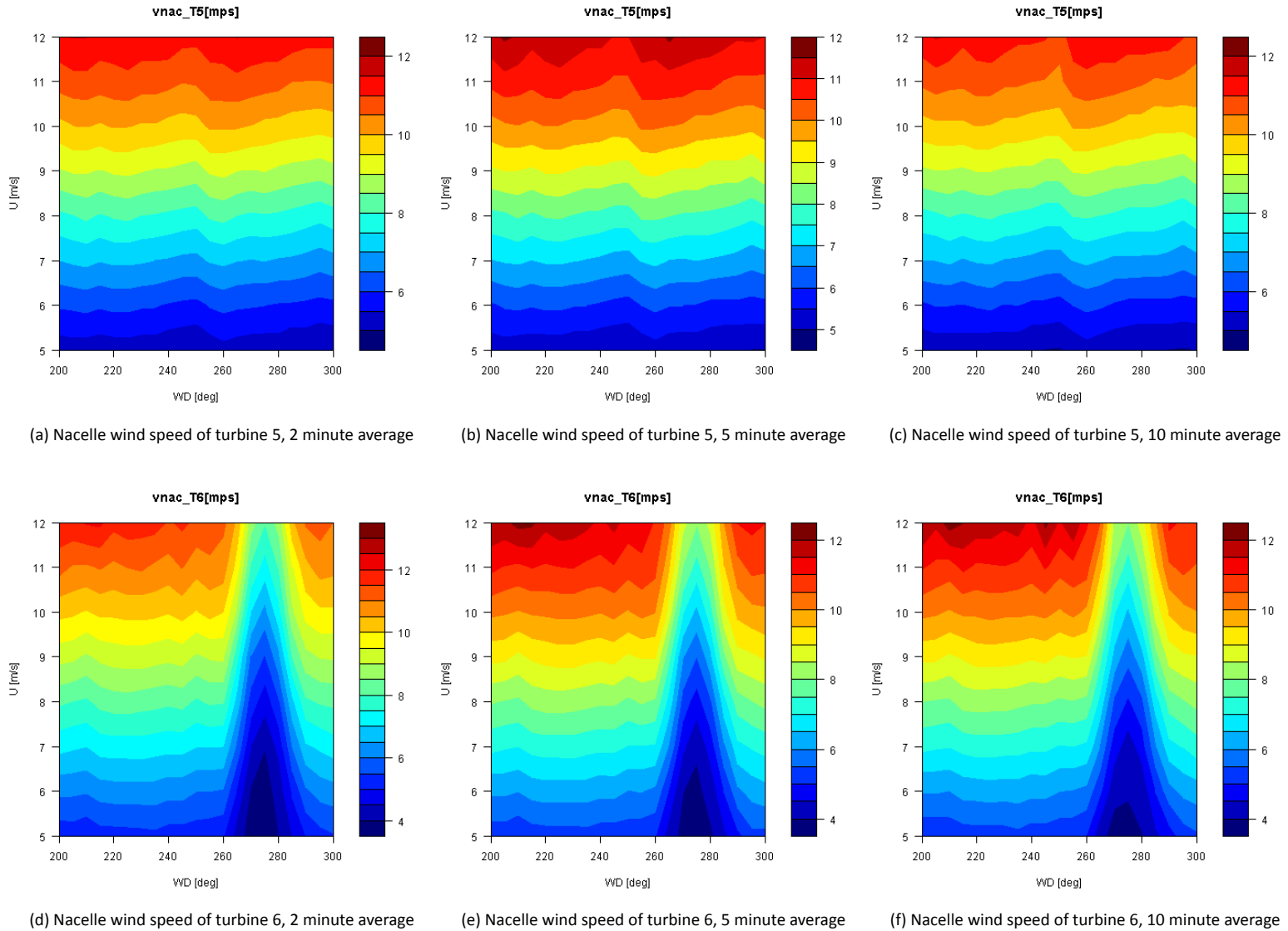


Figure 23: Nacelle wind speed of turbine 5 (above) and turbine 6 (below) for configuration 00xxx

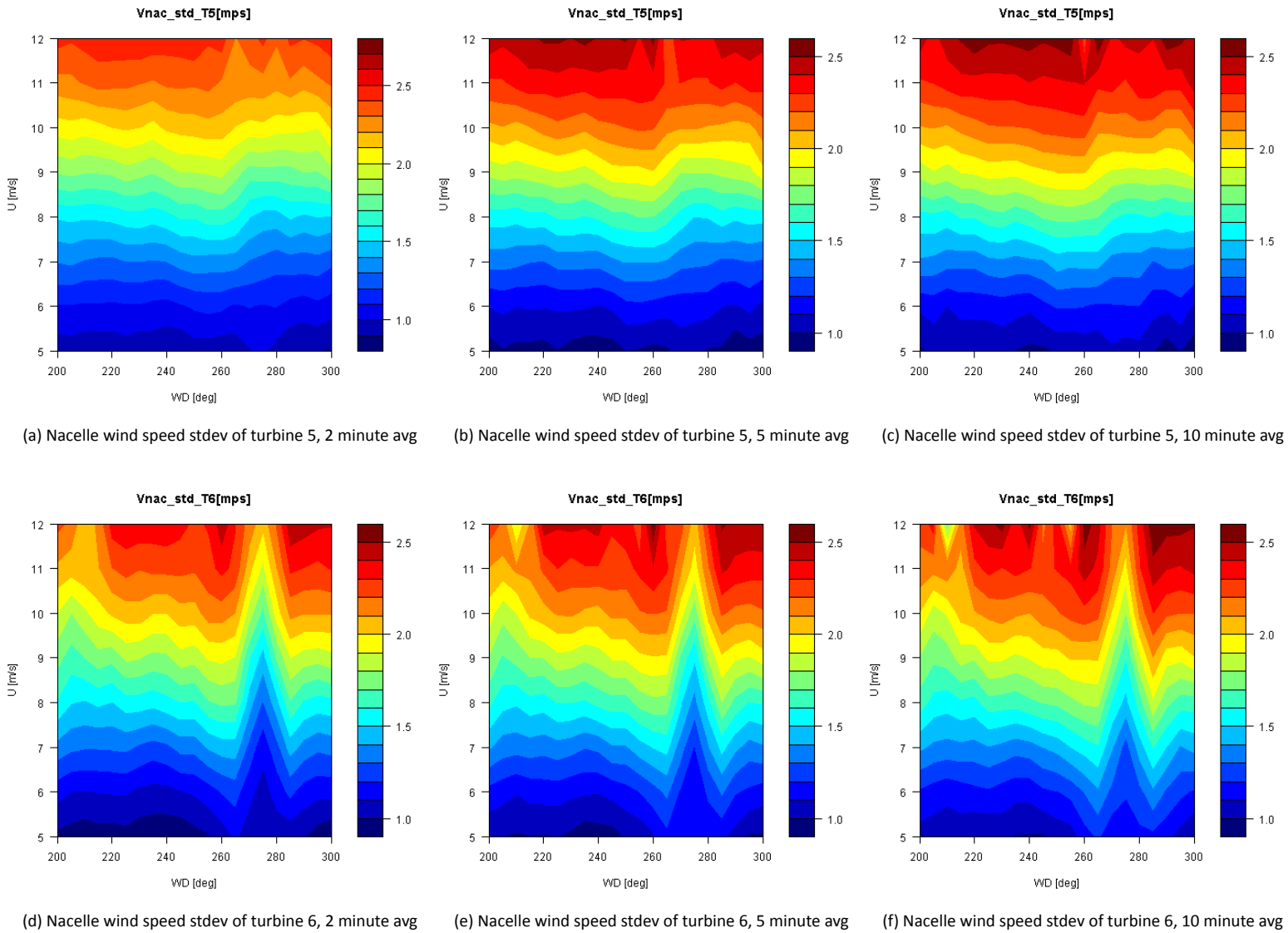


Figure 24: Nacelle wind speed standard deviation of turbine 5 (above) and turbine 6 (below) for configuration 00xxx

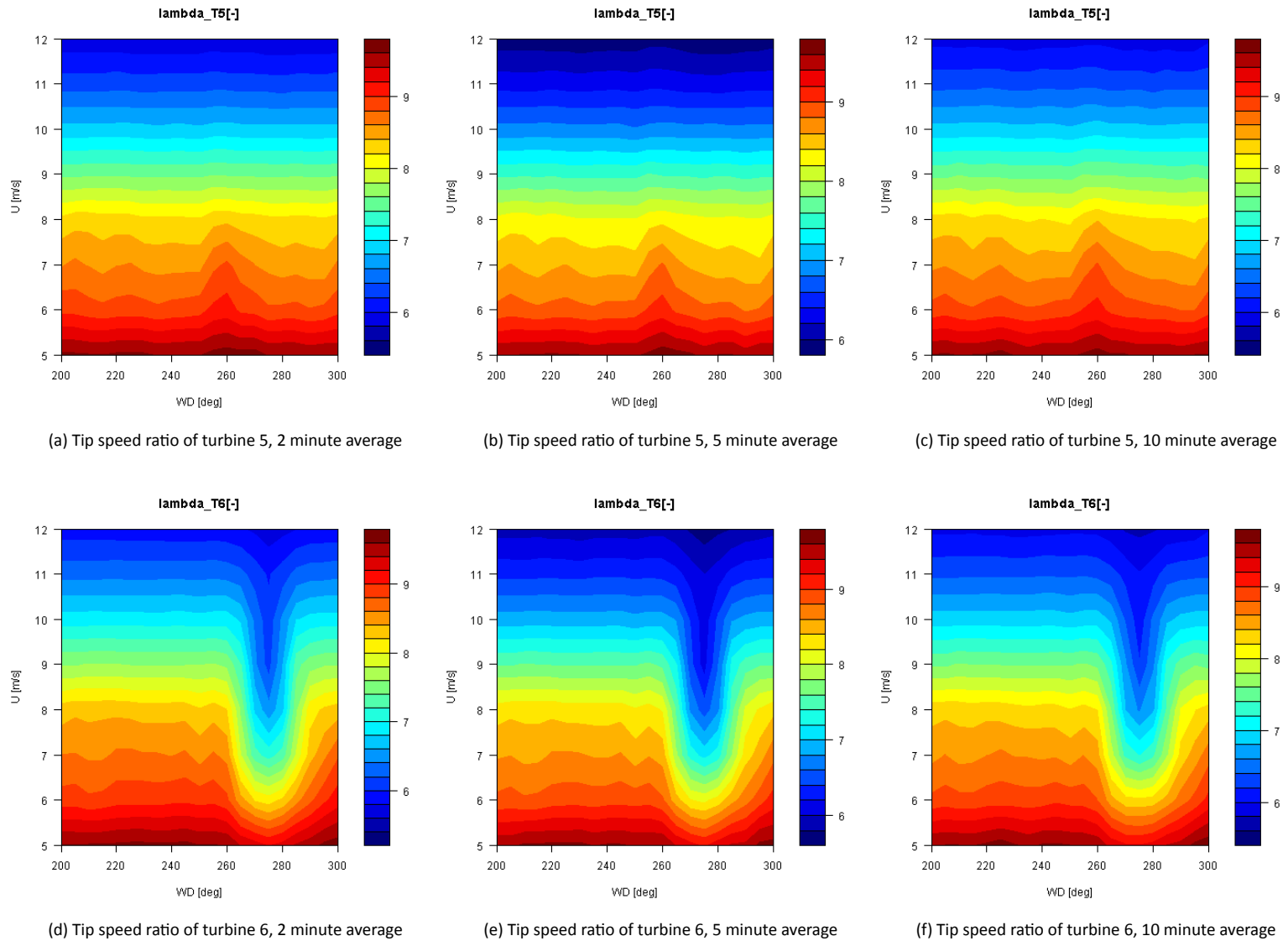
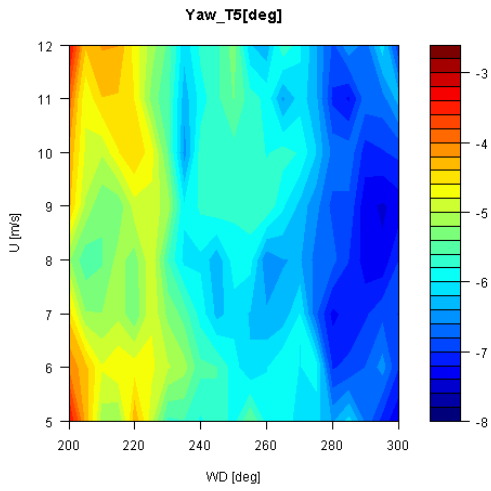
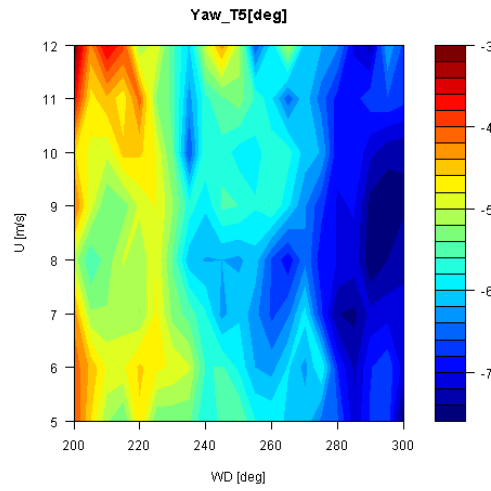


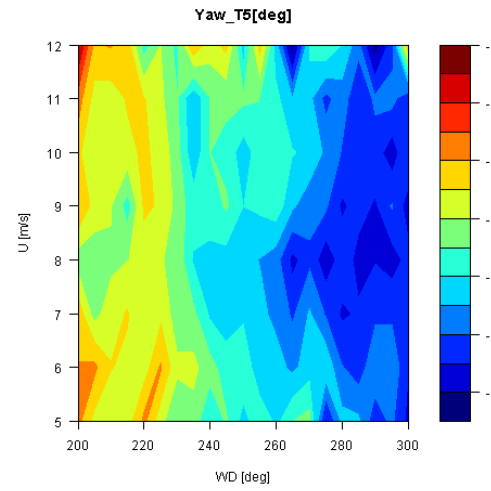
Figure 25: Tip speed ratio of turbine 5 (above) and turbine 6 (below) for configuration 00xxx



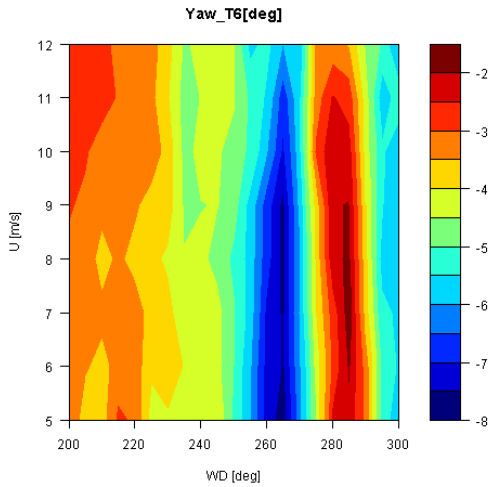
(a) Yaw angle of turbine 5, 2 minute average



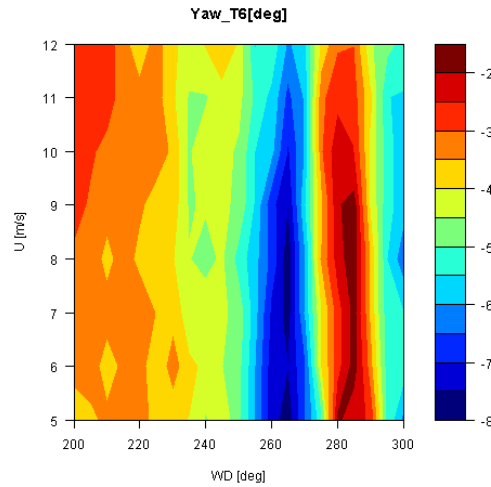
(b) Yaw angle of turbine 5, 5 minute average



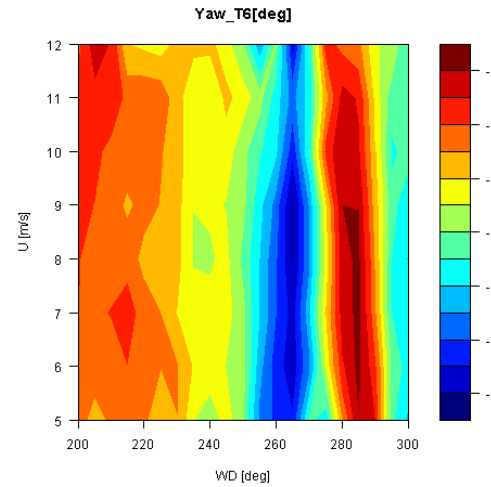
(c) Yaw angle of turbine 5, 10 minute average



(d) Yaw angle of turbine 6, 2 minute average



(e) Yaw angle of turbine 6, 5 minute average



(f) Yaw angle of turbine 6, 10 minute average

Figure 26: Yaw angle of turbine 5 (above) and turbine 6 (below) for configuration 00xxx

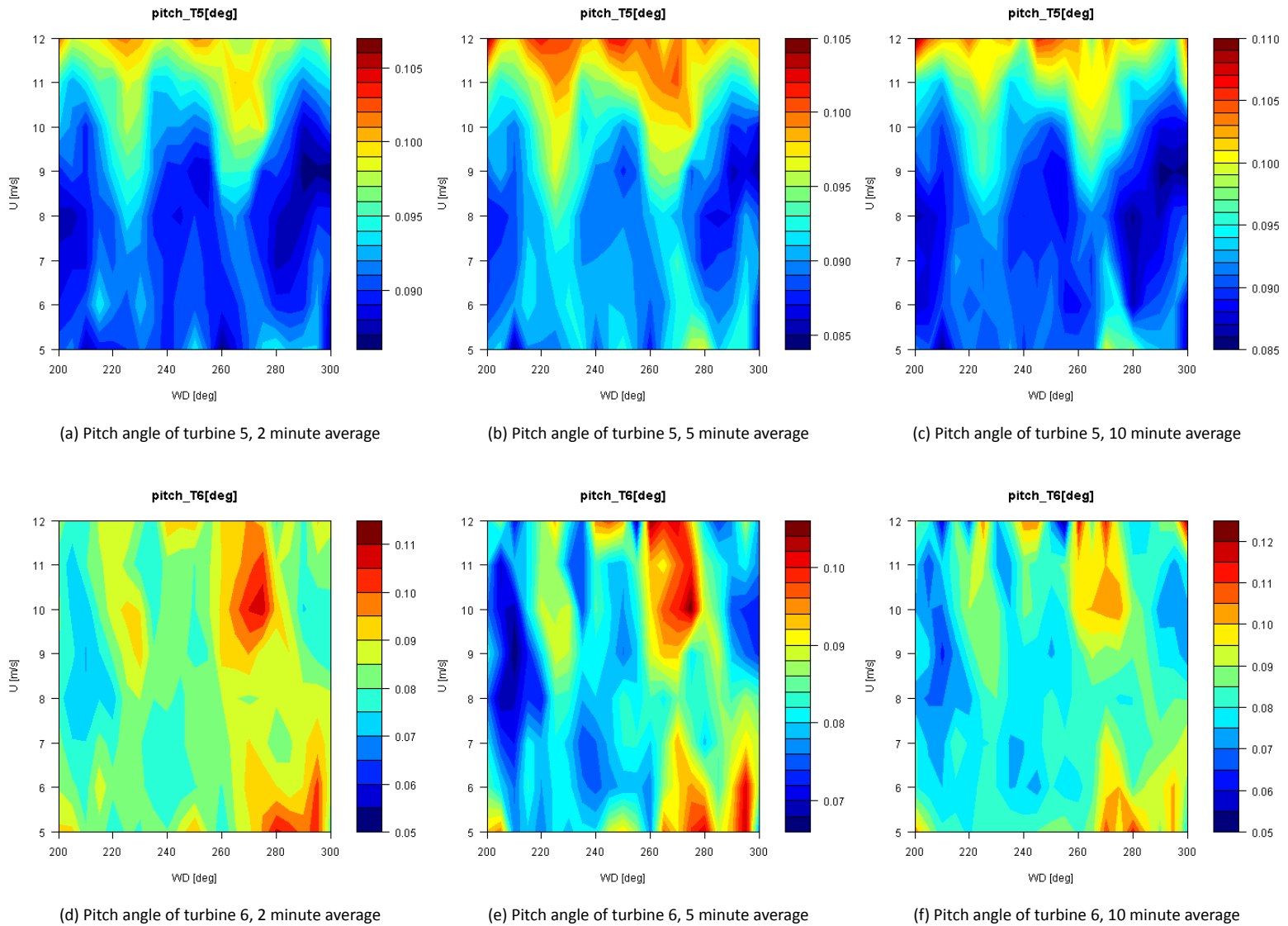


Figure 27: Pitch angle of turbine 5 (above) and turbine 6 (below) for configuration 00xxx



ECN

Westerduinweg 3
1755 LE Petten
The Netherlands

P.O. Box 1
1755 ZG Petten
The Netherlands

T +31 88 5154949
info@ecn.nl
www.ecn.nl